Universidade da Beira Interior
Ciências da Saúde

Isolation and purification of STEAP1 protein fragment in *Escherichia coli* cells: a potential target for prostate cancer

Jorge Daniel Barroca Ferreira

Dissertação para obtenção do grau de Mestre em
Ciências Biomédicas
(2º ciclo de estudos)

Orientador: Prof. Doutor Cláudio Jorge Maia Batista
Coorientador: Prof. Doutor Luís António Paulino Passarinha

Covilhã, junho de 2016

Acknowledgments

Firstly, I would like to thank to my supervisors, Professor Cláudio Maia and Professor Luís Passarinha for the opportunity that was given me to develop this project and for the constant availability to receive me, clear all my doubts and drive me through the best possible way. Also, thank to my colleagues at CICS for the support, mutual aid and for sharing a lot of headaches and endless hours of tough work.

To all my dear friends with whom I shared the greatest and the worse moments of my life during these last five years, and specially to my girlfriend, a huge thank for all the support and care. My boys and girls, believe that you had inspired me and were an extra motivation throughout this dissertation. A huge thank to Desertuna for being an important daily distraction outside the lab, for letting me relief stress over the most beautiful stages and places in Portugal, and essentially for preparing me to face the real world challenges.

There are no words to described my gratitude to my family, in special my mom and dad. Their daily effort for keeping me study all these years away from home and for always bringing a smile to my face through a special word of incentive and courage is priceless. I will never be able to return what you have done for me. This dissertation is entirely dedicated to you all.

Resumo

O cancro da próstata é o segundo tipo de cancro mais prevalente em todo mundo e a sexta causa de morte relacionada com a doença. As terapias atualmente aplicadas nomeadamente em estádios avançados não são completamente eficazes e apresentam diversas limitações. Por conseguinte, é necessário desenvolver alternativas recorrendo, por exemplo, a tecnologias vanguardistas que permitam identificar genes codificantes de proteínas membranares, abundantemente expressas em tecidos cancerígenos. *The six-transmembrane epithelial antigen of the prostate 1* (STEAP1) é uma proteína constituída por seis domínios transmembranares interligados por *loops* extracelulares, geralmente localizada na membrana plasmática, como por exemplo em junções de comunicação ou mesmo em membranas endossomais, sugerindo que atua como um canal membranar ou proteína transportadora ao nível da comunicação intercelular entre células tumorais. Em associação com a elevada especificidade e níveis de expressão significativos em tecidos cancerígenos prostáticos, a STEAP1 é um candidato promissor para ser imposto como alvo terapêutico, em especial para imunoterapia. No entanto, o facto de não ser possível a sua produção em quantidades significativas impede o desenvolvimento de estudos que permitam estabelecer a estrutura tridimensional e estudar o seu comportamento *in vivo*. Assim, os objetivos principais consistiram em definir o meio de cultura e as condições ótimas de fermentação para obter o máximo de rentabilidade na biossíntese do primeiro *loop* da STEAP1 ($STEAP1_{1-142}$), para além de avaliar diferentes condições inerentes ao método *immobilized metal affinity chromatography* (IMAC), de forma a obter níveis consideráveis de péptido purificado. Os resultados demonstraram que a fermentação em meio TB a 37 ºC, 250 rpm e pH 7.2 ao longo de 8 horas aumentou os níveis de biossíntese de $STEAP1_{1-142}$. O detergente Triton X-100 a 1 % (v/v) provou ser o mais eficaz ao nível da recuperação proteica, resultado validado por *Western-blot* pela presença de uma banda única imunorreativa com o peso molecular expectável (17-25 kDa). No passo de purificação foram testadas duas resinas carregadas com níquel e cobalto. Os resultados evidenciaram um típico perfil cromatográfico, no qual a proteína alvo foi completamente retida. No entanto, uma quantidade considerável de proteínas provenientes do hospedeiro *Escherichia coli* (*E. coli*) eluíram juntamente com o fragmento $STEAP1_{1-142}$, sendo necessário desenvolver uma estratégia alternativa de eluição e otimizar a pureza das frações alvo.

Palavras-chave

Cancro da próstata, proteínas membranares, STEAP1, produção de proteínas, IMAC.

Resumo alargado

O cancro da próstata é o segundo tipo de cancro mais prevalente em todo mundo e a sexta causa de morte relacionada com esta doença, apresentando especial incidência em homens situados numa faixa etária entre os 45 e 80 anos de idade. As terapias atualmente aplicadas no tratamento do cancro da próstata, nomeadamente em estádios avançados não são completamente eficazes e apresentam diversas limitações. Por conseguinte, é necessário desenvolver alternativas recorrendo, por exemplo, a tecnologias vanguardistas de biologia molecular que permitam a identificação de genes codificantes de proteínas membranares, abundantemente expressas em tecidos cancerígenos. *The six-transmembrane epithelial antigen of the prostate 1* (STEAP1) é uma proteína constituída por seis domínios transmembranares interligados por *loops* extracelulares, geralmente localizada na membrana plasmática, como por exemplo em junções de comunicação ou mesmo em membranas endossomais, sugerindo que atua como um canal membranar ou proteína transportadora ao nível da comunicação intercelular entre células tumorais. Em associação com a elevada especificidade e níveis de expressão significativos em tecidos cancerígenos prostáticos, a STEAP1 é atualmente um candidato mais promissor para ser utilizado como alvo terapêutico. No entanto, o facto desta proteína não ser até ao momento produzida em elevadas quantidades impede o desenvolvimento de estudos de biointeração, estruturais e construção de antagonistas. Assim, o primeiro objetivo deste trabalho passou pela construção do vetor de expressão pET101/D-STEAP1$_{1-142}$ e a posterior transformação da bactéria *Escherichia coli* (*E. coli*) BL21 (DE3). Posteriormente, foram testados diferentes meios líquidos de cultura (LB, TB, 2YT, SOC, SOB e semi-definido), com monitorização contínua do perfil de crescimento do hospedeiro e ainda definidas as condições ótimas de fermentação, considerando temperatura, agitação orbital e pH, com o intuito de alcançar o máximo de rendimento no processo de biossíntese do primeiro loop da STEAP1 (STEAP1$_{1-142}$). O passo seguinte consistiu em isolar o péptido de interesse no seu estado nativo adotando o método de lise por esferas de vidro, sendo que na etapa de solubilização foi estabelecido o detergente (SDS, Triton X-100, Tween-20, Digitonina, CHAPS) que melhor permitiu obter uma maior recuperação proteica. Após o vasto leque de estudos desenvolvidos, foi possível definir a cultura de *E. coli* BL21 (DE3) em meio TB a 37 ºC, 250 rpm e pH 7.2 ao longo de 8 horas, apresenta os níveis de de STEAP1$_{1-142}$ mais elevados, sendo o detergente Triton X-100 o que possibilitou uma maior solubilização da proteína de interesse. A análise por Wester- blot dos resultados alcançados evidenciou a presença de uma única banda imunorreativa com o peso molecular previsto para o nosso péptido de interesse (17-25 kDa), estando deste modo reunidas as condições para avançar com as etapas de purificação. Assim sendo, na etapa de purificação por I*mmobilized Metal Affinity Chromatography* (IMAC) foram testadas colunas carregadas com duas matrizes distintas, nomeadamente níquel e cobalto, avaliando-se a presença ou ausência de imidazole no tampão

de ligação e uma metodologia de gradiente linear de imidazole durante a etapa de eluição, na tentativa de obter níveis consideráveis de péptido purificado. No entanto, os resultados demonstraram ainda a presença de quantidades consideráveis de contaminantes, pelo que será necessário adotar estratégias alternativas para que num futuro próximo seja possível desenvolver estudos que permitam não só estabelecer a estrutura tridimensional, mas também estudos de biointeração para avaliar o comportamento *in vivo* do da $STEAP1_{1-142.}$

Abstract

Prostate cancer is the second most prevalent type of cancer worldwide and the sixth cancer-related death. The current applied therapies in advanced cancer stages are limited and not completely efficient. Thus, it is necessary to develop alternatives using, for example, molecular biology vanguard technologies that allow to identify genes that encode transmembrane proteins, abundantly expressed in cancer tissues. The six-transmembrane epithelial antigen of the prostate (STEAP1) was recognized as a protein presenting a structure with six transmembrane domains connected by extracellular loops. It is commonly located in plasma membrane, for example in communication junctions or even in endosomal membranes, suggesting a role as ion channel or transporter protein in intracellular communication between tumor cells. In association with its high specificity and significant expression levels in prostatic cancer tissues, STEAP1 is a promising candidate to be imposed as a therapeutic target, especially for immunotherapy. However, the impossibility of large-scale production hinders the development of structural and biointeraction studies, not only to establish the tridimensional structure of STEAP1 but also to understand its vivo behavior. Therefore, the main objectives consisted in establish the culture medium formulation and optimal fermentation conditions in order to achieve a maximum yield for the STEAP1 first loop ($STEAP1_{1-142}$) biosynthesis, besides access several conditions inherent to immobilized metal affinity chromatography (IMAC) to obtain considerable levels of purified peptide. The main results showed that TB medium fermentation at 37 ºC, 250 rpm and pH 7.2 over 8 hours increased the $STEAP1_{1-142}$ biosynthesis levels. Moreover, Triton X-100 at 1 % (v/v) demonstrated to be the most effective detergent for protein recovery. This result was validated by Western-blotting analysis which revealed a single immunoreactive band with the expected molecular weight (17-25 kDa). Concerning the purification step by IMAC, we tested two resins charged with nickel and cobalt. The results lead to a typical chromatographic profile where the target fragment was completed retained. Nevertheless, a considerable amount of heterologous proteins from *Escherichia coli* (*E.* coli) host co-eluted with the $STEAP1_{1-142}$ fragment, being necessary to develop an alternative elution strategy and optimize the purity of the target fractions.

Keywords

Prostate cancer, transmembrane proteins, STEAP1, protein biosynthesis, IMAC.

Index

List of figures

Figure 15: A: Chromatographic profile of STEAP1$_{1-142}$ purification from *E. coli* lysates on a HisTrap FF crude (5 mL column volume) with cobalt ions immobilized; B: Western blot/SDS-PAGE analysis of collected fractions. STEAP1$_{1-142}$ position in the western blot gel is at the correct position (17-25 kDa); C: STEAP1$_{1-142}$ fraction in SDS-PAGE gel (Comassie staining) is represented by an arrow. Blank line represents absorbance at 280 nm, while dashed line the imidazole concentration. Binding process was performed at 50 mM imidazole at 0.5 mL/min flow rate followed by an increasing elution linear gradient to 500 mM imidazole at 1.0 mL/min flow rate. A final step at 500 mM imidazole, 500 mM NaCl, 50 mM Tris and 1 mM MgCl2 buffer at pH 7.8 and 1.0 mL/ min flow rate was also observed.

List of tables

List of abbreviations

ABC	Adenosine triphosphate-binding cassette
ADT	Androgen deprivation therapy
AR	Androgen-receptor
ATP	Adenosine triphosphate
BPH	Prostatic hyperplasia
BSA	Bovine serum albumin
CHAPS	3-[(3-cholamidopropyl) dimethyl-ammonio]-1-propanesulfonate
COMT	Catecol O-Metiltransferase
CRPC	Castration-resistant prostate cancer
CTL	Cytotoxic T lymphocytes
CVs	Column volumes
CZ	Central zone
DHT	5α-dihydrotestosterone
DNA	Deoxyribonucleic acid
DNase	Deoxyribonuclease I
E. coli	*Escherichia coli*
E2	17ß-estradiol
EPCA	Early prostate cancer antigen
ETS	E26 transformation specific
EZH2	Enhancer of zeste homolog gene 2
FDA	United States Food and Drug Administration
GltP	Glutamate proton symporter
GnRH	Gonadotropin releasing hormone
GPCRs	G protein-coupled receptors
hSGLT1	Human sodium-glucose transport 1
HTL	Helper T lymphocytes
IMAC	Immobilized metal affinity chromatography
IPTG	Isopropyl-ß-D-1-thiogalactopyranoside
LB	Luria-bertani
LHRH	Luteinizing hormone-releasing hormone
mAb	Monoclonal antibody
MAPEG	Membrane-associated proteins in eicosanoid and glutathione
MCTs	Monocarboxylate transporters
NMR	Nuclear magnetic resonance
OD	Optical density
OD_{600}	Optical density at 600nm

PCa	Prostate cancer
PCA3	Prostate cancer antigen 3
PCR	Polymerase chain reaction
pET101/D	Champion™ pET101 Directional TOPO®
PIN	Prostatic intraepithelial neoplasia
PSA	Prostate specific antigen
PSCA	Prostate stem cell antigen
PSMA	Prostate specific membrane antigen
PVDF	Polyvinylidene difluoride
PZ	Peripheral zone
SDS	Sodium dodecyl sulfate
SDS-PAGE	Sodium dodecyl sulphate-polyacrylamide gel electrophoresis
SPR	Surface plasmon resonance
STD-NMR	Saturation-transfer difference NMR
STEAP	Six-transmembrane epithelial antigen of the prostate
TAA	Tumor-associated antigen
TB	Terrific-broth
TMPRSS2	Transmembrane protease serine 3
TZ	Transition zone
UGS	Urogenital sinus
YidC	Integral membrane chaperone
uPA	Urokinase plasminogen activator

Chapter 1

Introduction

1. Anatomy and Physiology of the Prostate

The development of the prostate begins at 10-12 weeks of gestation, being the first molecular modification the growth of prostatic bunds from its embryonic precursor, the urogenital sinus (UGS). It includes organ determination, epithelial budding, duct elongation, branching morphogenesis, cellular differentiation and maturation (1-4). The mutual interactions between the stromal and epithelial compartments are also crucial to initiate the postnatal development and maturation of the prostate (5).

The process inherent to prostate development is dependent on the action of sex steroid hormones that occurs in response to testicular androgen-mediated interactions, wherein the biological active 5α-dihydrotestosterone (DHT), derived from local conversion of fetal testosterone by 5α-reductase plays the main role (1-8). Testosterone also acts in order to maintain a totally differentiated epithelium with secretory functions, being then required for the maintenance of prostatic and glandular functions (4, 8).

After birth, serum testosterone levels decrease and the prostate stagnates its growth, weighing about 2g in childhood (4, 7). Only at puberty, its exponential growth due to augmented levels of androgens, secreted from the testes, stimulate the last morphofunctional changes needed to establish the adult phenotype, which is constituted by a multicellular mesenchymal layer surrounding secretory ducts with basal and luminal epithelial cells as well as neuroendocrine cells (2, 4, 5, 7). Until near 25 to 30 years of age, the prostatic weight remains similar and starts to rise slowly, reaching about 20 g, presenting a shape similar of a walnut and measuring 3 cm in length, 4 cm in width and 2 cm in depth (2, 6).

McNeal has established the most accepted model for the anatomy and physiology of the prostate. The adult male human prostate is composed by: i) peripheral zone (PZ), ii) central zone (CZ), iii) transition zone (TZ) and iv) the anterior fibromuscular stroma zone. This last structure is surrounded by a capsule of stromal fibromuscular tissue, within an inner layer of smooth muscular and an outer covered of collagen (2, 6, 9-13). Regarding the anatomic location, the prostate base is connected to the bladder neck, surrounding the proximal urethra in the anteromedial prostate, and the apex is under the urogenital diaphragm up to the midprostate, between the rectum and the symphysis pubis, in a subperitoneal region essentially composed by skeletal muscle fibers (2, 6, 10). The seminal vesicles constitutes an important accessory gland located superiorly to the prostate base, towards the vas deferens to form the

ejaculatory ducts, performing a connection with the vasa or ducti deferentia through a layer from the bladder muscle, also covering the prostate (2, 6).

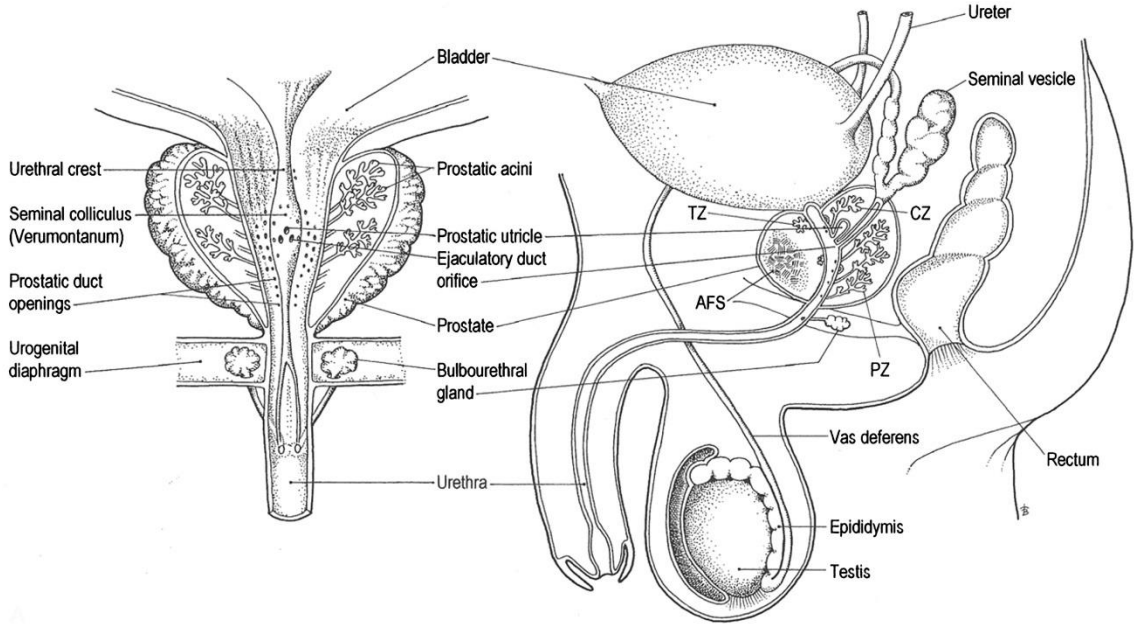

Figure 1: Diagrams of frontal and sagittal sections of the male urogenital complex, illustrating the anatomical position of the adult prostate and associated structures (14).

The glandular prostate comprises the UGS-derived PZ, which constitutes 65% of a normal organ mass and it is divided into an anterior and posterior branches, exiting posterolaterally from the verumontanum, in the urethral wall, to the prostate apex, wherein the carcinoma is more susceptible to occur (2, 9-12, 15). The CZ is a cone shape region derived from the Wolffian duct, comprising 30% of the total prostate mass, with ducts arising on the verumontanum and then projected to cover the confluence region of the ejaculatory ducts and the prostatic urethra (2, 9, 10, 15). The transition zone TZ encompasses only 5%, contains the urethral sphincter and a segment of the proximal urethra, from the verumontanum to the bladder neck, being also organized into two similar lobes of glandular tissue and muscle fibers, whose ducts leave the posterolateral gap of the urethral wall and extend laterally (2, 9, 11, 12, 16).

The anterior fibromuscular stroma has an apical half rich in striated muscle, converging into the prostate and muscles of the pelvic diaphragm, stimulating cell proliferation and presenting secretory functions, being also composed by a base predominant in smooth muscle cells, extending into the fibers of the bladder neck (1, 2, 4). The distal portion is relevant for the voluntary sphincter functions, whilst the involuntary ones are attributed essentially to the proximal region (2).

The main functions of the prostate consist in providing proteins, ions and nutrients needed for a correct composition of the prostatic secretions, which are then mixed with the fluids released from the seminal vesicles, creating the final ejaculate (4, 6). This is crucial in further processes

related to semen gelation, coagulation and liquefaction, in the coating and uncoating of spermatozoa and its interaction with cervical mucus, essential for the fertility success (4).

2. Prostate Cancer

Prostate cancer (PCa) is the second most prevalent type of cancer among man and the sixth leading cause of male cancer-related death worldwide (5, 17). In 2013, 238.590 new cases of PCa were diagnosed in man ranging 45 to 80 years of age and an estimated value of 29.729 patients died, particularly in underdeveloped countries (17, 18). The risk factors are a combination of endogenous factors, including hormones, aging, oxidative stress and exogenous, related to environmental risk factors, such as lifestyle habits, geographic residence area and socioeconomic standing (19-21). The genetic factors also has a direct role in the incidence of PCa and individual susceptibility to acquire this disease, mainly the family history and ethnicity, with special incidence in Afro-Americans, followed by Caucasians and Asians (3, 19, 20, 22).

PCa is divided into 2 different types, familial and sporadic. Familial disease is characterized by the appearance of cancer at early ages, less than 55 years old, in members of the same family. Sporadic PCa is triggered in cases when the genetic material is damaged by environmental constrains during life (20). The pathophysiology of PCa englobes benign lesions, namely benign prostatic hyperplasia (BPH) or malignant, such as prostatic intraepithelial neoplasia (PIN) or adenocarcinoma (23), as represented in figure 2.

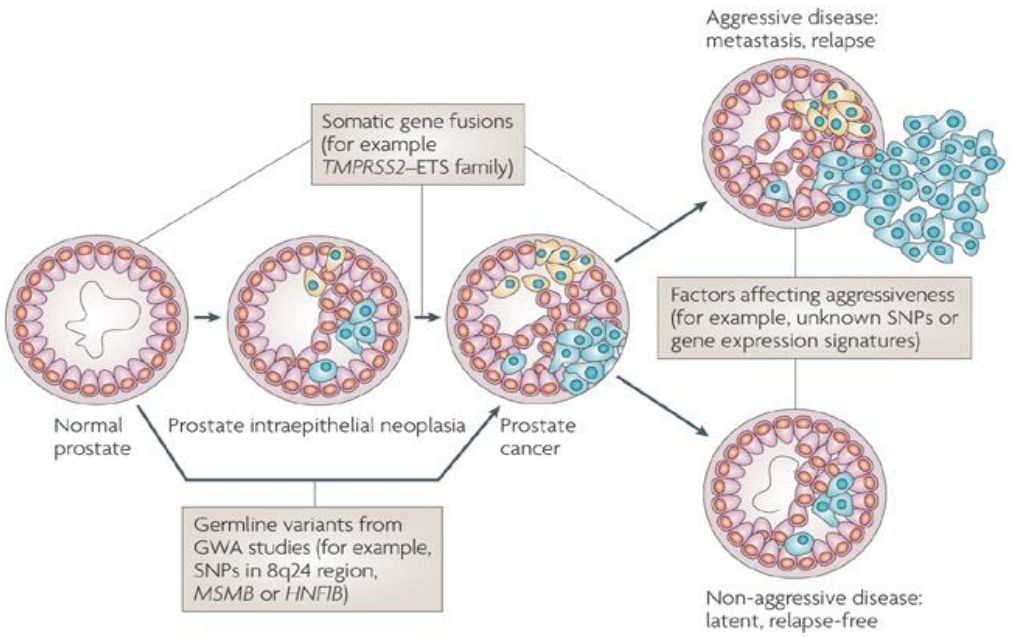

Figure 2: Progression pathway for human PCa, including pathological stages and the most relevant genetic alterations at each stage (24).

The tumor growth starts generally slow and asymptomatic and may involve an indolent course without metastatic disease development (25). As cancer develop, the prostate has multiple tumor foci that become progressively less organized, with smaller ducts, until occur a complete

loss of these structures (26). Likewise, gene expression is changed according to cancer stage and prostatic lesion type (27). Therefore, the cancer is capable to invade surrounding tissues and contribute to the development of metastasis (26, 27). Usually, cancer-related death is attributed to metastatic process, where tumor cells acquire the ability to spread from a primary to a secondary site. This is a complex process that includes the degradation of the basement membrane, the invasion, intravasation, anoikis evasion and extravasation of the extracellular matrix (28, 29).

2.1. The Role of Androgens in Carcinogenesis

The normal prostate cells are dependent of androgens, which maintain their growth, survival and terminal differentiation. In addition, androgens play an important role for the normal architecture, homeostasis and physiological function of the prostate (10, 30). The mechanism of androgens action is mediated through the androgen receptor (AR), which is expressed in several adult and fetal reproductive tissues, such as prostate, testis and seminal vesicle. The main androgen with biological action in the prostate is DHT, which presents higher affinity and activity than testosterone, and it plays both stimulatory and inhibitory roles in order to regulate the normal prostate growth and biologic functions (3, 5, 31-33).

The AR is a member of the nuclear steroid receptor superfamily of transcription factors, with a molecular weight of 110 kDa (30, 31). It is located on the X-chromosome (Xq11-12), composed up to eight exons, encoding approximately 919 amino acids, with different functional motifs namely an amino-terminal domain with a transactivation domain 1, crucial for the regulation of primary transcription, a DNA-binding domain containing two zinc fingers responsible for DNA recognition, dimerization and stabilization, which can be connected to the hinge region, being responsible for the regulation of receptor nuclear import through a nuclear localization signal. Moreover, it has a C-terminal domain, comprising a ligand binding domain and the transactivation domain 2, also involved in regulation of transcription (31, 34-36)

The initial state of AR is inactive, but becomes active when bound to DHT. Conformational changes allow AR dimerization, which is accompanied with the dissociation of cytoplasmic heat shock proteins, and consequently, it may translocate into the nucleus. Then, it binds to androgen-response elements within the gene regulatory region, stimulating or inhibiting the expression of several genes (31, 37-39).

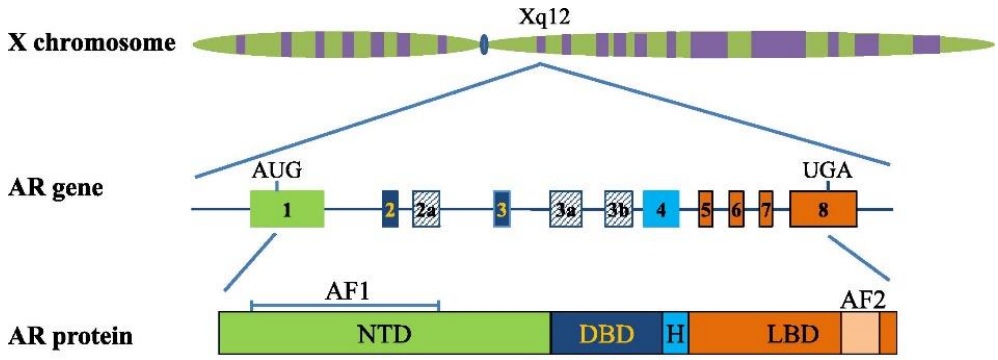

Figure 3: Schematic representation of the AR gene and protein structure (37).

In PCa cells, the AR is broadly expressed in the majority of initially diagnosed patients and the androgen/AR signaling axis has an active function in early stages of the disease. Taking into account the role of AR in cell proliferation, it is considered the main driver of prostate malignant cells development and progression (3, 5, 38, 40, 41). It is well documented that many patients will eventually become castration-resistant prostate cancer (CRPC), and there are several studies showing the involvement of AR, such as AR mutations, imbalance of AR co-regulators, alteration of selective androgen/AR signal transduction pathways and changes in the surrounding microenvironment and stromal cells or *de novo* synthesis (figure 3) (36, 38, 42).

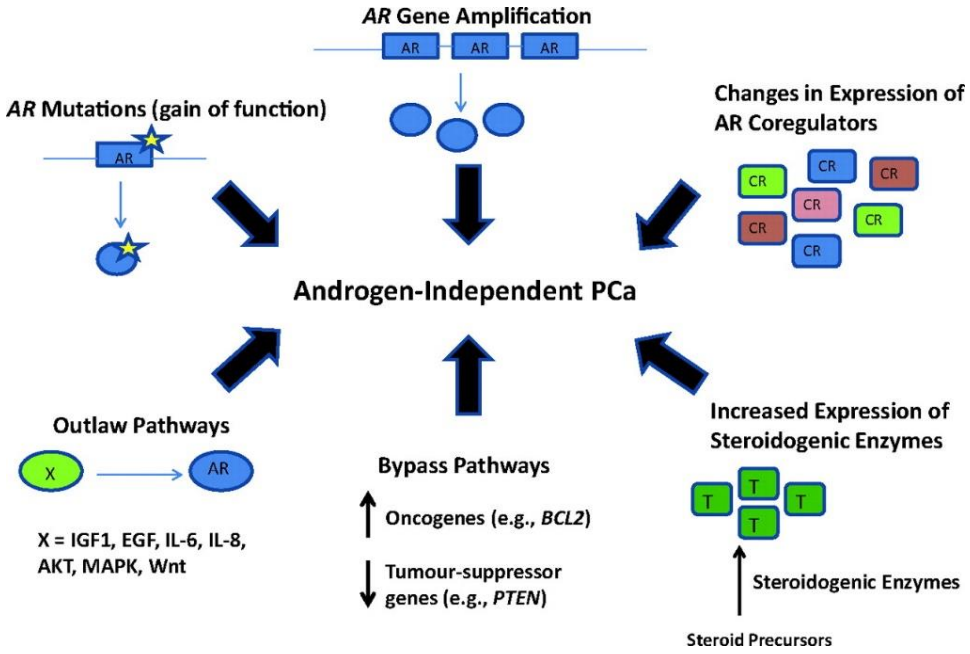

Figure 4: Mechanisms of androgen independence in PCa (38).

Actually, over 300 AR mutations have been identified in PCa patients and cancer cell lines, being its frequency and nature dependent on the cancer stage. In localized primary PCa, mutations of the AR are uncommon (0%-4%), but their frequency is significantly increased in advanced or metastasized profile (8, 38, 43, 44). The most relevant essentially result in

alteration or loss of AR function or represent a disruption of signaling pathways. Functional studies revealed a gain of function mutations, characterized by increased binding affinity and the consequent activation of the AR by estrogenic and progestagenic steroids, adrenal androgens and DHT metabolites. Cells carrying this type of mutations present a growth advantage in androgen-deprived environment, essentially due to alteration in cofactor recruitment and reduction of ligand specificity (38, 43-45).

The functional levels of androgens can be maintained through the conversion of adrenal androgens or intratumoral *de novo* synthesis of androgen, which is considered a relevant mechanism contributing to reactivate and restore the AR transcriptional activity (46, 47) Then, *de novo* synthesis of steroids in PCa cells is a possible reason for the progression into an castration-resistant profile, contributing to tumorigenesis in the absence of testicular androgens (5, 8, 38, 48).

2.2. Diagnosis and Treatment

At early stages, the prostate specific antigen (PSA) is used to detect patients with PCa, which is increased in serum levels (19, 20). However, there are several limitations because serum PSA levels may also be increased in cases of BPH (49). In addition, the quantity of PSA levels in serum are not capable to predict disease aggressiveness or if the tumor will progress into a metastatic stage (19, 50-52). Another diagnostic marker is the urinary prostate cancer antigen 3 (PCA3), which was firstly identified in 1999 as overexpressed in more than 95% of primary cancer tissues and associated with metastasis (53). Although there is a correlation between the PCA3 levels and PCa risk, it does not ensure tumor existence, since many cancerous patients may present low PCA3 levels (54, 55).

Therefore, it is needed to identify novel biomarkers to detect aggressive prostatic lesions. For that, several complementary methods are usually performed, including the screening of molecular differentiation between PCa stages, application of adjuvant therapies to enhance cancer regression, imaging techniques, trans-rectal examination with ultrasound guidance and biopsy (19). Together with the assessment of several clinical features of patients such as age, family history, tumor stage, serum PSA, Gleason score, number of positive prostate biopsies and the amount of malignant tissue, it is possible to establish a most suitable and appropriated treatment (19).

Usually, active surveillance is applied to patients with Gleason score of 6 or less, avoiding unnecessary or potentially harmful treatment, since this type of PCa is considered inoffensive. Regarding the PCa with low recurrence risk or in early stages, the primary treatment consists in radiation-based therapy or radical prostatectomy, which demonstrated to be effective in cancer reverse by destruction or excision of damaged tissue (19, 31, 38, 56). However, PCa can undergo recurrence and progress into a metastatic profile. In this context, the standard

treatment applied in the last 70 years has been surgical or chemical castration, also known as androgen deprivation therapy (ADT) (31, 57, 58).

Briefly, the ADT treatment consists in blocking the AR/androgen pathway or trigger an improperly activation of the AR, using radical radiotherapy as a complement. For that, it is necessary to submit patients to hormonal manipulations through androgen antagonists or agonists for gonadotropin releasing hormone (GnRH), which cause tumor shrinkage, retard it growth and progression, besides prevent testosterone production, based on the androgen dependency of prostate cells to survive. Surgical methods can also be applied, namely orchiectomy or chemically with luteinizing hormone-releasing hormone (LHRH) agonists, LHRH antagonists or anti-androgens in combination with castration by combined androgen blockade for reducing tumor burden and associated pain (31, 59-61). The newest upgrades on the biologic mechanisms underlying PCa allow to apply novel chemotherapeutic drugs approved for the United States Food and Drug Administration (FDA) as a complementary strategy, which have been effective in improving the survival time of man with advanced PCa, as summarized in table 1.

Table 1: Brief description of main FDA-approved drugs used to treat PCa and their respective effects.

Drug	Class	Effect	References
Abiraterone acetate	Androgen antagonist	Inhibit androgen biosynthesis Increase average survival time of patients Suppress testosterone concentration in tumor microenvironment	(19, 59-62)
Bicalutamide		Decrease pain Minimize sexual dysfunction Antitumor activity Improve cancer-associated symptoms	(19, 30, 61, 62)
Cyproterone acetate		Suppress androgen binding to AR Increase programmed necrosis	(19, 40)
Enzalutamide		Increase average survival time of patients Prevent nuclear translocation and chromatin binding of AR	(19, 60, 61)
Flutamide		Decrease PSA levels and relieve cancer-associated symptoms Suppress androgen binding to AR	(30, 37)
Cabazitaxel	Chemotherapeutic drug	Increase average survival time of patients Decrease PSA levels and relieve cancer-associated symptoms	(19, 60, 62)
Docetaxel		Increase average survival time of patients Decrease PSA levels and relieve cancer-associated symptoms	(19, 39, 60, 62)
Leuprolide	GnRH agonist	Persistent stimulation of pituitary gland Suppression of testosterone production	(57, 60)
Goserelin			(56)
Lupron	LHRH agonist	Diminish androgen levels in local cancerous tissues	(63)

Despite the initial PCa remission induced by ADT, this therapy is not completely efficient in eradicate the entire population of affected cell, besides negatively select subpopulations that survive in the absence of androgens. Moreover, after 2 to 3 years of treatment, a significant percentage (10%-40%) of patients experience disease relapse and starts to progress into widespread metastasis or transit from the initial androgen-dependent state to CRPC, which is characterized by the maintenance of the AR signaling and expression of AR-regulated genes, and it is also associated with a poor prognosis and short survival time (37-39, 60, 64).

Considering that the current established therapies are limited and induce side effects that impairs the life quality of patients, it is necessary to develop alternatives, which should be more effective and less toxic, in order to manage those who develop recurrent disease or present advanced tumor stage or metastatic disease. Therefore, innovative molecular biology

technologies, including differential display analysis, subtraction approaches and microarrays, which allow to identify several genes that encode transmembrane proteins (65, 66).

The discovery of novel membrane protein commonly founded in several human pathologies are nowadays a promising tool for a deeper understanding of biologic mechanisms underlying the diseases. Consequently, it is possible to perform a thorough study of relevant interactions relaying the target protein and 3D structure analysis. The ultimate goal is to develop therapeutic drugs with high binding affinity or design a proficient therapy capable to manage and revert the injurious effects induced by its overexpression in human tissues.

2.3. Transmembrane Proteins over-expressed in Prostate Cancer

The prostate-specific membrane antigen (PSMA) was identified in 1987 as a type II integral membrane glycoprotein overexpressed in PCa epithelial cells involved in hydrolyzing peptides in prostatic fluids (65, 67). It can be used to follow the progress of the disease in a posttreatment phase due to considerable sensitivity and specificity in distinguish PCa from other type of malignancies or as a target for monoclonal antibodies (mAb) (65).

The prostate stem cell antigen (PSCA) is a prostate-specific glycosyl phosphatidylinositol-anchored glycoprotein expressed on the cell surface, being its increased levels related with PCa presence, stage, progression and metastasis (65, 68). Despite its function is still unclear, PSCA may play a role in progenitor cell function, tumorigenesis and clinical progression (67).

The early prostate cancer antigen (EPCA) is a nuclear structural protein associated with PCa presenting high sensitivity and specificity, suggesting its use as a significant biomarker (65, 69). The function of EPCA is still unknown, however it is suggested a relation with and early step in prostate carcinogenesis (67).

The enhancer of zeste homolog gene 2 (EZH2) is a member of the polycomb group of proteins, commonly overexpressed in PCa and promoter of cancer growth. EZH2 acts as a gene silencer by maintaining the transcription repressive state of genes. However, it also silences the expression of tumor suppressor genes triggering an increased overexpression in metastatic PCa, in comparison with localized and BPH (65, 67). Therefore, it could be useful as a biological marker to identify patients at risk of metastasis (70).

The urokinase plasminogen activator (uPA) axis represents a potential target for PCa due to its involvement in various phases of tumor development and progression (65, 71) Consequently, its raised levels are correlated with cancer stage and metastatic onset (65).

The transmembrane protease serine 2 (TMPRSS2) regulates the overexpression of E26 transformation-specific (ETS) transcription factors, which are considered a persistent feature

in approximately 50% of patients, and are involved in PCa progression by disrupting AR signaling (20, 65, 72).

The monocarboxylate transporters (MCTs), particularly MCT2 and MCT4, are transmembrane proteins with consistent overexpression in the majority of androgen unresponsiveness PCa, being then considered important biomarkers that allow to distinguish between affected tissues from non-neoplastic (73-75). Likewise, some general markers can also be correlated with PCa, including N-cadherin which provides information for PCa treatment, since it predicts cancer recurrence after ADT and also ZEB1, being its overexpression correlated with high Gleason scores (65, 76, 77).

Table 2: Description of main biomarkers for PCa and their respective functions.

Marker	Description	Function	References
PSMA	Type II integral membrane glycoprotein	Hydrolyze peptides in prostatic fluids Follow the progress of the disease in a posttreatment phase Target for monoclonal antibodies	(65, 67)
PSCA	Prostate cell suface-specific glycosyl phosphatidylinositol-anchored glycoprotein	Related with cancer presence, stage, progression and metastases Progenitor cell function, tumorigenesis and clinical progression	(65, 67, 68)
EPCA	Nuclear structural protein	Early prostate carcinogenesis	(65, 67, 69)
EZH2	Polycomb group of proteins	Promote cancer growth Gene silencer Biomarker for metastatic patients	(65, 67, 70)
uPA	Serine protease	Cancer development and progression	(65, 71)
TMPRSS2			(20, 65, 72)
MCTs	Transmembrane monocarboxylate transporter	Biomarker for unresponsiveness PCa	(73-75)

ADAM9 and CDON are also found overexpressed in PCa, despite the last present low specificity. Therefore, only ADAM9 is considered a therapeutic targets for PCa, contrary to CDON that need more studies regarding expression and function in human cancer (66, 78). Nowadays, the six-transmembrane epithelial antigen of prostate 1 (STEAP1) is considered the most proper candidate to be imposed as a potential therapeutic target, since it fulfills all the desirable characteristics, namely high expression associated with a high PCa specificity (66, 79).

3. Six Transmembrane Epithelial of the Prostate 1

The STEAP family comprises four members, namely STEAP1 to STEAP4, sharing a similar structure with six transmembrane domains, edged by a carboxy- and an amino-terminal intracellular domains (80-82). The majority of STEAP proteins has an YXXØ (in which Ø is a large hydrophobic amino acid) consensus sequence and the Rossman fold (GXGXXG/A motif) responsible for targeting transmembrane proteins to lysosomes and endosomes. These domains are intrinsic characteristics of proteins with oxidoreductase and dehydrogenase functions, respectively, and have the ability to bind nucleotides such as NAD and FMN (80, 81). Despite all the common features and high homology degree between STEAPs, their cellular functions, expression patters and subcellular localization are distinct (81, 82).

STEAP1 gene is located close to the telomeric region at the long arm of chromosome 7q21.13, includes 5 exons and 4 introns along 10.4 kb size and contains a gene cluster predicted to encode transmembrane proteins. The transcription mechanism origins 2 different mRNA of 1.3 kb and 4.0 kb (80, 81, 83). However, only the first one is translated into a protein with 399 amino acids and a molecular weight of 39.72 kDa (80-83).

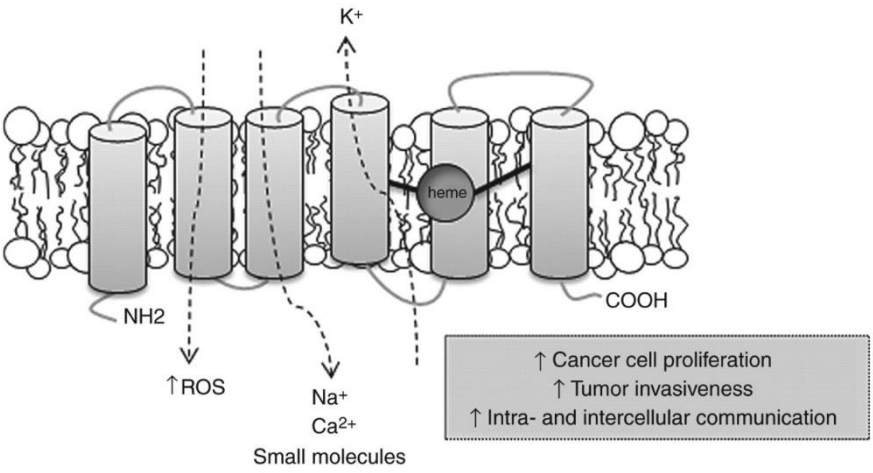

Figure 5: Schematic of STEAP1 protein structure, cellular localization, and pathophysiologic functions (80)**.**

STEAP1 is not homologous to any other familiar proteins, since its structure suggests that it is a cell-surface molecule composed by six-transmembrane domains with the COOH- and N-terminals located in the cytosol, 3 extracellular and 2 intracellular loops (80, 84, 85). The transmembrane domains are located at 73-95, 117-139, 164-182, 218-240, 252-274, 289-311 base pairs of the amino acid sequence (83). In contrast with the other proteins, STEAP1 lacks N-terminal NADPH-oxidoreductase, FNO-like domain and Rossman-fold, turning it the smallest of the classical STEAPs (80-82, 86). Additionally, this protein keeps two conserved histidine residues implicated in FRE heme-binding proteins and contains a flavin-NADPH-binding domain, despite structurally distinct and located at C-terminal (87). It also presents another heme-

binding domain called “apoptosis, cancer and redox associated transmembrane”, which facilitates the transmembrane electron transfer, and consequently, affects cell growth and its metabolism, as represented in figure 5 (25, 88).

Concerning the ferric oxidoreductase activity of STEAP1, it contributes to the generation, metabolism and increased levels of intracellular reactive oxygen species (ROS), which induces the expression of redox-sensitive and pro-invasive genes (80, 81, 83, 86, 89). In addition, it activates several signaling pathways involved in metastatic and proliferative cancer cells. Thus, the upregulation of ROS-levels, as a consequence of STEAP1 overexpression, is a hallmark of several cancers, including PCa (86, 89).

3.1. Expression and Function in Human Tissues

STEAP1 is highly expressed in several types of human cancers as well in cancer cell lines, namely in prostate, bladder, breast, colon, cervix, ovary, pancreas, testis and Ewing sarcoma (80, 84, 86, 90). The expression of STEAP1 is almost restricted to the prostate gland, mainly at cell-cell junctions located in the plasma membrane of prostate epithelial cells or in basal layer, which may behave as a prostate stem cells reservoir (23, 80). Although at very low levels, this protein is also present in non-tumoral tissues such as breast, colon, fallopian tubes, pancreas, pituitary, stomach, ureter and uterus (83, 84, 90).

The primary location of this protein is in the columnar epithelial cells at the apical plasma membrane of cell-cell junctions, besides being also dispersed in the cytoplasm and endosomal membranes (84, 90, 91). Herein, it plays a role in iron metabolism caused by the ubiquitous expression and partial co-localization with transferrin, transferrin receptor 1 and endosomes, which are specialized in iron and cooper uptake (82, 86). Therefore, due to its location and secondary structure, STEAP1 acts as an ion channel or transporter protein in both tight and gap junctions or even in cell adhesion processes, playing an important role in intracellular communication between tumor cells and surrounding stromal cells (79, 84, 90). Likewise, it has the capability to modulate the proliferation and invasion of cancer cells through the adjustment of intracellular concentration of few ions such as Na^+, K^+, Ca^{2+} and then triggering an enhanced effect in cell growth and, consequently in cancer development (79, 80, 92).

The cellular localization and expression patterns of STEAP1 may depend on histologic diagnosis (25, 84). Regarding BPH lesions, this protein is found in basal cells, while in PIN lesions it is located in luminal, basal and stroma cells (23, 25, 84). High levels of STEAP1 are associated with worse prognosis in PCa, being associated with cancer recurrence and aggressiveness (25).

STEAP1 constitutes an important target for bisphosphonates, since they are capable to reduce cell viability, in a dose-dependent manner and also decrease STEAP1 mRNA expression in PCa cells, due to its cytostatic effects (93, 94). During the last few years, the use of bisphosphonates in PCa increase exponentially, since this compounds are capable to inhibit cancer cells growth,

adhesion and invasion processes (95, 96). As Zoledronic Acid is the most powerful amino-bisphosphonate, which exerts its action by reducing cell proliferation or inducing cell apoptosis through low and high doses, respectively (97).

A similar study showed that a prolonged exposure to zinc induces an aggressive behavior of PCa cells, therefore enhancing tumor cells proliferation and simultaneously increasing the expression of STEAP1 genes (98). In normal prostate gland, zinc is highly expressed and it is essential for normal functions of prostate cells. On the other hand, this compound is significantly reduced in prostate malignancies and any alteration in its homeostasis triggers an uncontrolled growth of tumor cells and leads to cancer development. This is essentially due to an impairment in the expression of regulatory genes in several biologic processes and signal transduction pathways, regulated by zinc (98-100).

Considering the role of sex steroid hormones in PCa, STEAP1 regulation was evaluated by DHT and 17β-estradiol (E2) in LNCaP cells. Surprisingly, STEAP1 expression decrease in time- and dose-dependent manner in both cases. However, this effect is not mediated by their cognate receptors, and thus it is possible that the levels of STEAP1 decrease in response to sex steroid hormones in order to overcome the proliferation effects triggered by these hormones (91). Therefore, cells presenting higher expression levels of STEAP1 have a more aggressive behavior, confirming a relationship between with the AR at transcriptional level, which is reinforced by the genetic or pharmacologic suppression of STEAP1 mRNA by AR inhibitors (72, 101, 102).

Expectations about immunotherapy have been raising, transforming this practice a more attractive and achievable. Herein, it is crucial to establish human cancer and cancer-associated cytotoxic T lymphocytes (CTL) lines, which represent only the anergized immune system and trigger a cancer-specific response (103). However, the absence of tumor-associated antigen (TAA) capable of inducing this sort of response constitutes the central problem and invalidate the development of effective immune-based therapies (104).

3.2. Therapeutic Target

As referred before, STEAP1 expression levels in human PCa are 5- to 10- fold higher, comparing to other cancer types. Also, considering the location of STEAP1 in cell membrane associated to its low or absent expression in normal tissues, its epitopes became strong tools to develop novel methodologies focusing human cancer and a potential target for immunotherapy (84, 85, 103-105).

Likewise, cancer immunotherapy mainly occurs through immunogenic binding epitopes, and some studies have demonstrated that $STEAP1_{86-94}$ and $STEAP1_{262-270}$ are capable to stimulate antigen-specific CTL and helper T lymphocytes (HTL). Therefore, CTL and HTL recognize and destroy STEAP1-expressing cancer cells via TAA recognition mechanism, without elicit any significant autoimmune response (19, 103-105). Therefore, this is a promising method because

consists in a noninvasive option to treat minimal residual disease, to prevent metastatic spread, to inhibit the growth of prostate cancer cells or even to delay recurrences without compromising life quality (104). Nowadays, Sipuleucel-T is an active cellular immunotherapeutic agent constituted by antigen-presenting cells and several study cases demonstrated that it increase the average survival time of cancerous patients (19, 106, 107).

DNA vaccines are another promising tool for immunotherapy due to their ability to induce a highly specific T cell response and simultaneously capable to overcome the immune system surveillance and tolerance mechanisms employed by cancer cells (108-110). Several vaccines were already used against overexpressed proteins in PCa, including STEAP1, with genes encoding cytokines or co-stimulatory molecules to enhance the specificity of the immune response. The results obtained demonstrated that these vaccines induce a delay or even a inhibition in tumor progression (110, 111).

Nowadays, antibody-based therapies have become a preferred choice for targeting cancer. STEAP1 immunogenicity encouraged the development of antibody-drug conjugates, combining anti-STEAP1 specific mAb with chemotherapeutic drugs with cytotoxic potential or a detectable label agent to be used as therapeutic approach (112). The connection between anti-STEAP1 mAbs and external loops of the protein suppresses its biological function and thereafter compromises all the oncogenic functions (79, 101, 113). The mAb needs to bind preferentially to malignant cells at a relatively high density, and internalize in a manner that allows for release of the drug from the linker in the appropriate intracellular compartment. The linker needs to attach the drug to the mAb in a manner that is stable in the circulation, but releases the drug once it is internalized. The cytotoxic drug needs to be nontoxic when linked to the mAb in the circulation, but capable of killing tumor cells once it is internalized and released (114).

Moreover, its capacity to recognize antigens with a high selective degree specific, creates the idea of targeting malignant cells whit minimal undesired collateral toxicity to normal tissue, as it is proven by the successful mAb: trastuzumab, rituximab, cetuximan and bevacizumab (79, 101, 114, 115). Recently, novel anti-STEAP1 mAbs with stronger binding capacity and higher affinity to cell surface epitopes were capable to immunoprecipitate STEAP1 protein, modulate its functions as transporter through the blockage of intercellular communications and induced a significant inhibition of tumor growth (79). Also, a recent technology consisting in a novel diagnostic agent, consisting in a mAb radiolabeled complex immunoreactive for full-length human STEAP1 was capable to accumulate itself in the bloodstream at tumor site and detect precisely metastatic cells (101).

Currently, STEAP1 is not produced and isolated in considerable amounts to perform complementary structural studies, which constitute a significant limitation. In order to overcome this barrier, the information about post-translation modifications and predicted 3D

structure are achieved through *in silico* analysis. Once established the optimized conditions for STEAP1 production, techniques such as X-ray crystallography, circular dichroism, protein nuclear magnetic resonance (NMR), saturation-transfer difference NMR (STD-NMR), surface plasmon resonance (SPR) could be applied to provide complete information regarding STEAP1 crystalized structure and unspecific interactions (116-121).

4. Aims

To our best knowledge, there are no published studies in the literature focusing the implementation of a laboratory hands-on platform from the biosynthesis to purification of the $STEAP1_{1-142}$ immunodomain. A most effective manner to manage harmful effects of overexpressed STEAP1 levels in human PCa can be achieved by understanding the interactions between $STEAP1_{1-142}$ purified extracts and immunotherapeutic agents. For that, it is necessary to develop a biotechnology procedure capable of producing significant amounts of $STEAP1_{1-142}$ with considerable purity levels.

The main goals of this master thesis were:

- Construct the pET101/D-$STEAP1_{1-142}$ expression vector and transformation of E. *coli* BL21 (DE3) host;
- Define ideal culture medium formulation and optimal fermentation conditions to achieve maximum $STEAP1_{1-142}$ yield;
- Discover $STEAP1_{1-142}$ cellular compartmentalization;
- Isolate the $STEAP1_{1-142}$ in its native state from heterologous system and establish the most effective detergent for protein recover concerning the solubilization step;
- Develop IMAC chromatographic profiles in order to obtain considerable levels of purified $STEAP1_{1-142}$ for further biointeractions studies and 3D structure resolution.

Chapter 2

Materials and Methods

1. Materials

Ultrapure reagent-grade water was obtained with a Mili-Q system as well as lactose from Merck Millipore (Darmstadt, Germany). Agar and European bacteriological agar were acquired from Laboratorios CONDA (Madrid, Spain). Tryptone and yeast extract were obtained from BIOKAR Diagnostics (Allonne, France) Dipotassium phosphate, lysozyme and sodium dodecyl sulfate (SDS) were bought from AppliChem (Darmstadt, Germany). Monopotassium phosphate, magnesium chloride, magnesium sulfate, acid-washed glass beads, digitonin, ampicillin (sodium salt), isopropyl-ß-D-1-thiogalactopyranoside (IPTG) and deoxyribonuclease I (DNase) were purchased from Sigma-Aldrich (St. Louis, MO, USA). Sodium chloride, glucose, tris base, Triton X-100, Tween 20, methanol and acetic acid glacial 99 % were acquired from Fisher Scientific UK (Loughborough, UK). Potassium chloride was obtained from Panreac (Barcelona, Spain). Glycerol was obtained from HiMedia Group (Mumbai, India). 3-[(3-cholamidopropyl) dimethyl-ammonio]-1-propanesulfonate (CHAPS) was acquired from AMRESCO (Solon, OH, USA). The NZY ladder VI and NZYColour protein marker II for estimation of peptide base pairs (bp) and mass, respectively and GreenSafe Premium were purchased from NZYTech (Lisbon, Portugal). All other chemicals were of analytical grade commercial available and used without further purification.

2. Strains, plasmids and media

The *Escherichia coli* (*E.* coli) TOP10F' (Invitrogen, Carlsbad, USA) cells were used for deoxyribonucleic acid (DNA) manipulations. The *E. coli* transformants were selected on Luria-Bertani (LB) plates (10.0 g/L tryptone, 5.0 g/L yeast extract, 10.0 g/L sodium chloride, 35.0 g/L agar, pH 7.5) supplemented with 100 µg/mL ampicillin at 37 ºC. The plasmids pIRES-STEAP1 and pET101/D-hCOMT were applied on this purpose, while the pET101/D-STEAP1 was used as expression vehicle in *E.* coli BL21-Star (DE3) (Invitrogen) host. These cells were used for protein production in typical complex media, such as LB (10.0 g/L tryptone, 5.0 g/L yeast extract, 10.0 g/L sodium chloride, pH 7.5), SOB (20.0 g/L tryptone, 5.0 g/L yeast extract, 0.25 g/L sodium chloride, 10.0 mL/L magnesium chloride 1 M, 10.0 mL/L magnesium sulfate 1 M), SOC (20.0 g/L tryptone, 5.0 g/L yeast extract, 0.5 g/L sodium chloride, 0.2 g/L potassium chloride, 20.0 mL/L glucose 1 M, 10.0 mL/L magnesium chloride 1 M), 2xYT (8.0 g/L tryptone, 5.0 g/L yeast extract, 5.0 g/L sodium chloride) and Terrific-Broth (TB) (12.0 g/L tryptone, 24.0 g/L yeast extract, 4.0 mL/L glycerol, 100.0 mL/L fermentation salts, pH 7.2). All media were supplemented with ampicillin 100.0 µg/mL.

3. Construction of the pET101/D-STEAP1$_{1-142}$ expression vector

The Champion™ pET101 Directional TOPO® (pET101/D) expression kit (Invitrogen) was used for the expression of human STEAP1$_{1-142}$ peptide in its native form, according to manufacturer's instructions. Briefly, DNA fragment with approximately 500 bp coding for STEAP1$_{1-142}$ was cloned into another vector used as template for polymerase chain reaction (PCR). pET101/D-STEAP1$_{142}$ was constructed by PCR in T100™ Thermal Cycler (Bio-Rad, Hercules, USA) using specific cloning primers (forward primer: 5'-AAGG AATT CAGG AGCC CTTC ACCA TGGA AAGC AGAA AAGA CATC-3'; reverse primer: 3'-AATG AGCT CCTA ATGG TGAT GGTG ATGT GCAT GAAG TTGG ACAA TTGA TGCT-5') with EcoR I and Sac I restriction site for directional cloning. PCR was conducted in the following conditions: initial denaturation at 95ºC for 5 minutes, 30 cycles denaturation at 95 ºC for 30 s, annealing for 65 ºC for 30 s and extension at 72 ºC for 1 min and final elongation step at 72ºC for 5 minutes. The amplified cDNA fragment was confirmed by agarose gel electrophoresis and purified using NZYMiniprep kit (NZYTech). Previously, we digested STEAP1$_{1-142}$ with EcoR I (Takara Bio Inc., Shiga, Japan) and Sac I (Takara Bio Inc.) and then cloned into pET101/D, also digested with the same restriction enzymes, by T4 DNA ligase (NZYTech) over 4 hours. This construct was transformed into *E. coli* TOP10F' cells, grown overnight at 37 ºC in LB-Agar plates containing 100 µg/mL ampicillin and colonies were screened by PCR. Several positive colonies were inoculated in 4.0 mL of LB medium and grown overnight at 37 ºC and 250 rpm. From these cultures, highly purified plasmids were extracted using NZYMiniprep kit and subsequently subjected to DNA sequence analysis to confirm the identity of the target gene.

4. *Escherichia coli* transformation and selection of positive clones

Since the target plasmid pET101/D-STEAP1$_{1-142}$ was confirmed to correspond to human STEAP1$_{1-142}$, it was introduced into *E.* coli BL21-Star (DE3) competent cells, used as host for STEAP1$_{1-142}$ overexpression under the effect of ampicillin as a selection marker. Cell lyse of a single half colony at 95 ºC for 10 min was previously performed and the transformation process was carried out using 2 µL of a sequenced positive plasmid pET101/D-STEAP1$_{1-142}$ per 40 µL vial host solution. Furthermore, cells were plated in LB agar containing 100 µg/mL ampicillin and grown overnight at 37 ºC. High expression level of transformants were screened by PCR, conducted with the specific cloning primers (forward primer: 5'-AAGG AATT CAGG AGCC CTTC ACCA TGGA AAGC AGAA AAGA CATC-3'; reverse primer: 3'-AATG AGCT CCTA ATGG TGAT GGTG ATGT GCAT GAAG TTGG ACAA TTGA TGCT-5') using the following conditions: initial denaturation at 95ºC for 5 minutes, 30 cycles denaturation at 95 ºC for 30 s, annealing for 65 ºC for 30 s and extension at 72 ºC for 1 min and final elongation step at 72ºC for 5 minutes. The amplified DNA was assessed by agarose gel electrophoresis. The other colony half was inoculated in 62.5 mL LB pre inoculum medium, supplemented with 100 µg/mL ampicillin and cells were grown at 37ºC and 250 rpm overnight. The inoculation volume was fixed to achieve an initial cell density at 600nm (OD_{600}) equal to 0.2, measured by spectrophotometry (Pharmacia Biotech, Ultrospec 3000, Denmark) and a specific pre inoculum volume was transferred to 62.5 mL LB inoculum medium, also containing 100 µg/mL ampicillin. These values were calculated considering the mathematical

formula:

$$V pre\ inoculum \times \mathrm{OD} pre\ inoculum = \mathrm{OD} inoculum \times (V pre\ inoculum + \mathrm{V} inoculum)$$

These cells grown at 37ºC and 250 rpm, until OD_{600} reach the phase between 0.6 and 0.8. At this moment, a solution containing 70% inoculum medium with pET101/D-STEAP1$_{1-142}$ plasmid and 30% glycerol was prepared. Then, it was divided into criostem tubes and stored frozen at -80.0ºC until further use.

5. Biosynthesis of the STEAP1 fragment

Initially, cells containing the expression plasmid were grown at 37ºC in LB plates. Then, several colonies were inoculated in 25.0 mL of LB, S.O.B, S.O.C, 2xYT and TB media in 100-mL shake flasks. In initial assays, cells were grown at 37ºC and 250 rpm until OD_{600} reached 2.6. The inoculation volume was fixed to achieve an initial OD_{600} of 0.2 and the fermentations were conducted until an OD_{600} ranging 0.6-0.8. At this moment, IPTG and lactose were added to a final concentration of 1 mM, in 1000 mL shake flasks. The bacterial growth profile was accessed till stationary phase. Once established the ideal fermentation conditions, the studies were focused on TB medium, over 8 hours of fermentation without applying any inducer. An additional test considering previous results obtained in a semi-defined medium by Silva and coworkers, was performed applying the predicted temperature and stirring rate ideal conditions of 35 ºC and 351 rpm, respectively (122). Finally, cells were harvested by centrifugation (3500 g, 20 min, 4 ºC) and stored frozen at -80.0 ºC until use.

6. Cell lysis and STEAP1$_{1-142}$ solubilization

The bacterial cells pellet was resuspended in appropriate lysis buffer (500 mM NaCl, 50 mM Tris, 1 mM $MgCl_2$, pH 7.8) and disrupted by 0.5 mg/mL lysozyme treatment during 15 min at room temperature and mechanical action of acid-washed glass beads adapted from a previously defined ratio (1 g cellular mass : 2 g glass beads : 2 mL lysis buffer) (123). The mixture was vortexed 7 times for 1 min with an interval of 1 min on ice. Then, 0.10 mg/mL DNase I was added to the lysate immediately followed by centrifugation (16000g, 30 min, 4 ºC). After the centrifugation step, the solubilization was carried out incubating the 16000g pellet (P16000g) in 1% (v/v) Triton X-100 plus lysis buffer at 4 ºC overnight, until full solubilization. The 16000g supernatant (S16000g) was also collected, in order to understand the protein cellular compartmentalization, moment when these samples were discarded. In addition, four detergents namely SDS, Tween-20, CHAPS and Digitonin were tested for P16000 solubilization in order to compare their efficiency in STEAP1$_{1-142}$ fragment recovery. The samples were conserved at -80 ºC until further purity and immunoreactivity analysis by SDS-PAGE and Western-blotting, respectively. The protein contents were measured by Pierce BCA Protein Assay Kit (Thermo Fisher Scientific) using BSA as standard and calibration control samples according to the manufacturer's instructions.

7. STEAP1$_{1-142}$ purification in immobilized metal ion affinity chromatography

All chromatographic separation assays were performed at room temperature on ÄKTA avant purifier system with UNICORN 6.1 software (GE Healthcare) and all buffers pumped in the system were prepared with Mili-Q system water, filtered through a 0.20 µM pore size membrane (Schleicher Schuell, Dassel, Germany) and degassed ultrasonically. Two different Immobilized Metal Ion Affinity Chromatography (IMAC) commercial HisTrap™ FF crude 5 mL columns (GE Healthcare) were packed according to company guidelines with two distinct metals, nickel and cobalt.

In initial trials, the columns were equilibrated with binding buffer (500 mM NaCl, 50 mM Tris-base, 1 mM $MgCl_2$, 5 mM Imidazole, pH 7.8). Then, aliquots containing STEAP1$_{1-142}$ resuspended pellet in binding buffer (diluted 1:2) were injected onto the column using 2 mL at a 0.5 mL/min flow rate along 5 column volumes (CVs). The elution undergone through a linear gradient using an elution buffer (500 mM NaCl, 50 mM Tris-base, 1 mM $MgCl_2$, 500 mM Imidazole, pH 7.8) of 0 % to 100 % imidazole at 1.0 mL/min flow rate over 5 CVs. A final elution step was maintaining during approximately 2 CVs to perform a complete elution of the bounded. In all chromatography assays, pH profile, absorbance at 280 nm, conductivity and pressure were continuously monitored. The fractions of 2-6 mL corresponding to peak 1 and 2 were collected in Pierce™ Protein Concentrator PES (3.000 MWCO) and then concentrated at 4 ºC. The samples were conserved at -80 ºC until further purity and immunoreactivity analysis by SDS-PAGE and Western-blotting, respectively. The protein contents were measured by Pierce BCA Protein Assay Kit (Thermo Fisher Scientific) using BSA as standard and calibration control samples according to the manufacturer's instructions.

8. Agarose gel electrophoresis

The DNA electrophoresis was performed on a gel containing 1% agarose (GRiSP, Oporto, Portugal) and carried out in Tris-acetic acid (TAE) buffer (40 mM Tris base, 20 mM acetic acid and 1 mM EDTA, pH 8.0). The run undergoes at 120 V for 30 min and the bands corresponding to STEAP1$_{1-142}$ DNA, containing Green Safe reagent, were visualized under ultra violet (UV) light after using UVITEC FireReader (UVItec, Cambridge, UK).

9. Total protein quantification

The protein content in samples was measured by the Pierce BCA Protein Assay Kit (Thermo Fisher Scientific, Waltham, MA, USA), using bovine serum albumin (BSA) as the standards (0.025-2.0 mg/mL), according to manufacturer's instructions in xMark™ Microplate Absorbance Spectrophotometer (Bio-Rad). The lysis buffer curve was applied to quantify solubilized STEAP1$_{1-142}$ pellets while elution buffer curve was used for purified samples.

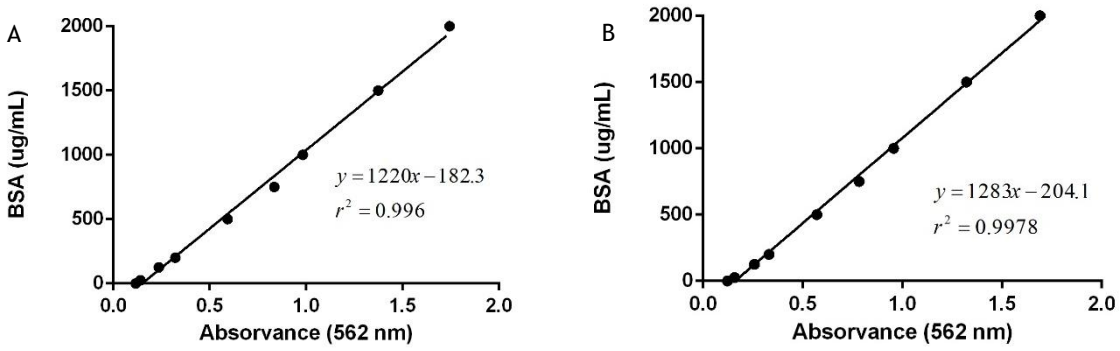

Figure 6: A - BSA (lysis buffer) calibration curve; B - BSA (elution buffer) calibration curve.

10. SDS-PAGE and Western Blot Analysis

A total protein mass ranging 2 µg and 5 µg were submitted to reducing sodium dodecyl sulphate-polyacrylamide gel electrophoresis (SDS-PAGE). Samples were boiled in loading buffer containing 500 mM Tris-Cl (pH 6,8), 10 % (w/v) SDS, 0.02 % bromophenol blue (w/v), 0.2 % glycerol (v/v), 0.02 % ß-mercaptoethanol (v/v) for 5 min and then run on 12.5 % stacking and resolving acrylamide (GRiSP) gels containing 0.1 % SDS, with a running buffer (25 mM Tris, 192 mM glycine, 0.1 % (w/v) SDS) at 120 V for 105 min. Then, one gel was stained by Coomassie brilliant blue overnight at room temperature over constant stirring followed by 1 h period in discoloration solution I (320 mL/L methanol, 56 mL/L acetic acid glacial 99%) and overnight in discoloration solution II (50 mL/L methanol, 70 mL/L acetic acid glacial 99%) at same conditions. The other gel was electrotransferred to a polyvinylidene difluoride (PVDF) membrane (GE Healthcare, Buckinghamshire, UK), for 30 min at 4 ºC in a buffer containing 10 mM CAPS and 10 % (v/v) of methanol. Subsequently, the membranes were blocked with washing buffer containing 5 % (w/v) milk for 60 min at room temperature and incubated overnight at 4 ºC with rabbit anti-STEAP1 at 1:300 dilution in washing buffer (Santa Cruz Biotechnology, Dallas, TX, USA) polyclonal primary antibody, followed by an incubation with an anti-rabbit IgG alkaline phosphatase secondary antibody at a 1:40000 dilution in washing buffer (Santa Cruz Biotechnology). The PVDF membranes were incubated with ECF substrate (GE Healthcare) for 5 min and immune-reactive proteins were detected by exposure to chemiluminescence detection with the Molecular Imager FX Pro Plus MultiImager (Bio-Rad).

Chapter 3

Results and Discussion

1. Construction of the pET101/D-STEAP1$_{1-142}$ expression vector

The construction of the pET101/D-STEAP$_{1-142}$ expression vector started with gene amplification by PCR, previously inserted in the plasmid pIRES/STEAP$_{1-142}$. Herein, it was important to determine the most appropriated annealing temperature, since it is a relevant factor that highly affects PCR reactions. Thus, several reactions were conducted using specific cloning primers for STEAP1$_{1-142}$ gene (forward primer: 5'-AAGG AATT CAGG AGCC CTTC ACCA TGGA AAGC AGAA AAGA CATC-3'; reverse primer: 3'-AATG AGCT CCTA ATGG TGAT GGTG ATGT GCAT GAAG TTGG ACAA TTGA TGCT-5'), at different annealing temperatures, namely 60 ºC, 62º C and 65º C. As represented in figure 7A, a DNA fragment with approximately 500 bp was amplified in all reactions, being lanes I, II and III correspondent to PCR reactions with annealing temperatures at 60 ºC, 62 ºC and 65 ºC, respectively. Since the density of each band raised with a temperature augment, we established the annealing temperature of 65 ºC for further assays.

Consequently, the amplified STEAP1$_{1-142}$ fragment was digested with EcoR I and separated from the vector in an agarose gel electrophoresis, from which the target DNA was purified using NucleoSpin: Nucleic Acid and Protein Purification kit. Thereafter, both STEAP1$_{1-142}$ insert and the vector pET101/D were digested with the restriction enzymes EcoR I and Sac I and the target fragment was cloned into pET101/D vector using T4 DNA ligase at several ratios vector/insert DNA over 4 h at room temperature. Then, E. *coli* TOP10 competent cells were transformed with the constructed plasmid by heat shock of 1 h in ice and 1 min at 42 ºC. These cells were inoculated overnight at 37 ºC in LB-agar plates supplemented with ampicillin and the grown colonies were picked, lysed at 95 ºC for 10 min and inoculated at least 16 h in 4.0 mL in LB-broth medium, also containing ampicillin, at 37 ºC and 250 rpm. Therefore, highly purified plasmids were prepared using a NZYMiniprep kit and an enzymatic digestion was performed to analyze the results in agarose gel electrophoresis, as reported in figure 7B. The plasmid contained the STEAP1$_{1-142}$ was properly digested, as shown by the amplified DNA fragment in each lane with approximately 500 bp, which should to correspond to the DNA fragment that encodes STEAP1$_{1-142}$.

In order to confirm the identity of DNA fragment cloned into the pET101/D vector, the plasmid was sequenced with T7 primers. After an analysis with BLAST program it was confirmed that DNA fragment encodes correctly the human STEAP1$_{1-142}$. Then, E. *coli* BL21 (DE3) cells were transformed with pET101/D-STEAP1$_{1-142}$ plasmid. Cells were inoculated overnight at 37 ºC in LB-

agar plates with ampicillin and the grown colonies were once again picked and lysed at 95 ºC for 10 min. In order to confirm the transformation process and the plasmid integrity, a PCR reaction was performed. As shown in figure 7C, an amplification with approximately 500 bp was visualized demonstrating that E. *coli* BL21 (DE3) host cells are transformed with pET101/D-STEAP1$_{1-142}$.

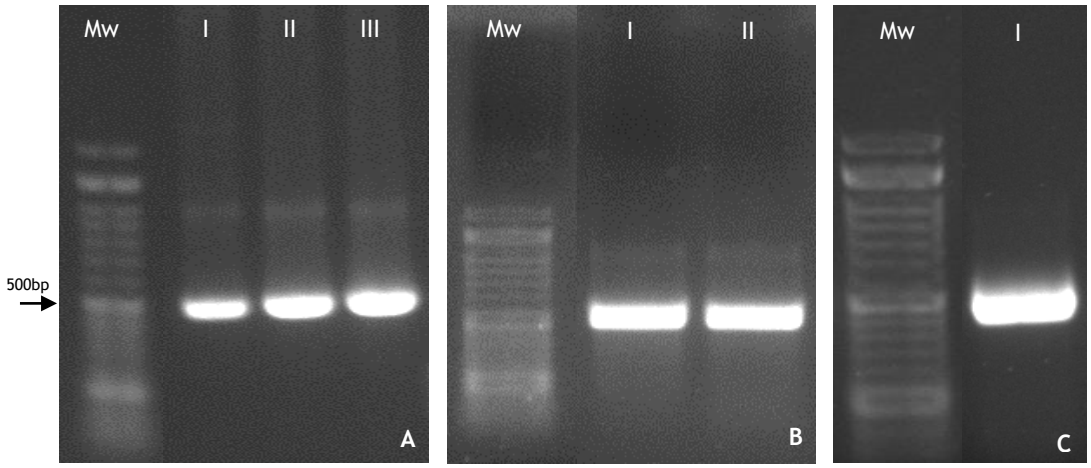

Figure 7: Agarose gel electrophoresis of two critical moments during the construction of the expression vector pET101/D-STEAP1$_{1-142}$. A: PCR products of STEAP1$_{1-142}$ amplification at different annealing temperatures, 60 ºC, 62 ºC and 65 ºC, respectively; B: Highly purified plasmid pET101/D-STEAP1$_{1-142}$ from *E. coli* TOP10 competent cells; C: Highly purified pET101 vector cloned with STEAP1$_{1-142}$ DNA insert from *E. coli* BL21 (DE3).

2. STEAP1$_{1-142}$ biosynthesis

Bacteria such as *E. coli* has been widely used as cellular host and considered one of the most valuable expression system for human proteins, since it presents a quick growth rate, allows highly levels of the target protein in a convenient, safer, cost-wise and less time-consume manner, in comparison with other recombinant systems (124-126). Despite not being commonly described in literature, *E. coli* has successfully been used for the heterologous expression of eukaryotic membrane proteins with relevance to drug discovery, including G protein-coupled receptors (GPCRs), membrane-associated proteins in eicosanoid and glutathione (MAPEG) family members and transporters, such as human sodium-glucose transport 1 (hSGLT1) protein and adenosine triphosphate (ATP)-binding cassette (ABC) transporters (124).

In this work, STEAP1$_{1-142}$ peptide was produced in prokaryotic organism *E. coli* BL21 (DE3), harboring the plasmid pET101/D-STEAP1$_{142,}$ previously described as a strain capable to overexpress functional human proteins, including single protein domains (127-129). Nevertheless, the media formulation for culturing *E. coli* cells does not require any specific components for a sustainable growth, an overview of the optimum culture conditions for overexpression of the target protein were conducted by testing culture medium composition and fermentation conditions, namely temperature, stirring rate and pH.

Firstly, the time course profiles of host growth were analyzed each hour by measure of OD_{600} in LB, TB, SOB, SOC and 2YT liquid media, along with pre inoculum cells grown at 37 ºC and 250 rpm, until OD_{600} reached 2.60. As reported in figure 8, the growth profile concerning LB and 2YT cultures appeared very time consuming besides presented lower OD_{600} levels. Therefore, as this behavior could negatively affect the yield of the target protein, these media were excluded.

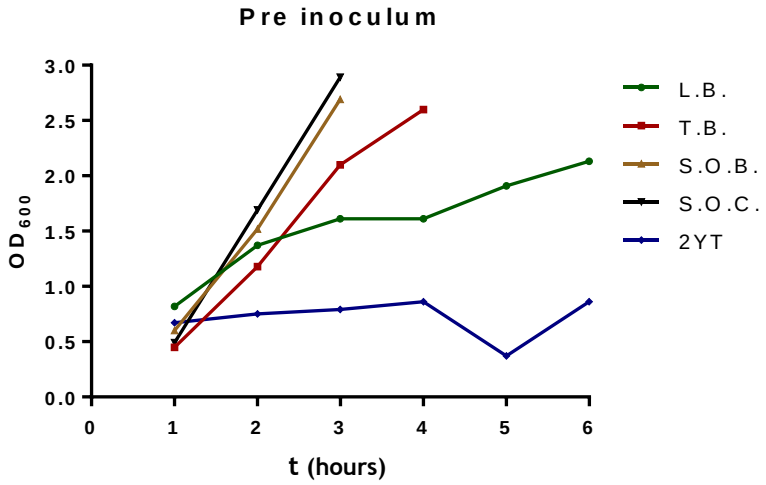

Figure 8: *E. coli* BL21 (DE3) growth profile of pre-inoculum cells in LB, TB, SOB, SOC and 2YT liquid culture media.

A recent study demonstrated that it is possible to efficiently produce membrane proteins in *E. coli* BL21 (DE3), without adding IPTG (130). As the influence of an inducer is actually poorly studied in an integrated and comparative manner, it was simultaneously evaluated $STEAP1_{1-142}$ biosynthesis in the presence and absence of IPTG in TB, SOB and SOC liquid media. As induction is recommended to initiate under exponential phase of the host, IPTG 1mM was added to cell culture and the growth profile was continuously monitored by the same methodology described above, up to stationary phase. The results obtained showed that, excepting SOC medium, E. *coli* fermentation profile was similar, with increasing OD_{600} over 8 h of fermentation, moment when this parameter stagnate or even decrease (Figure 9).

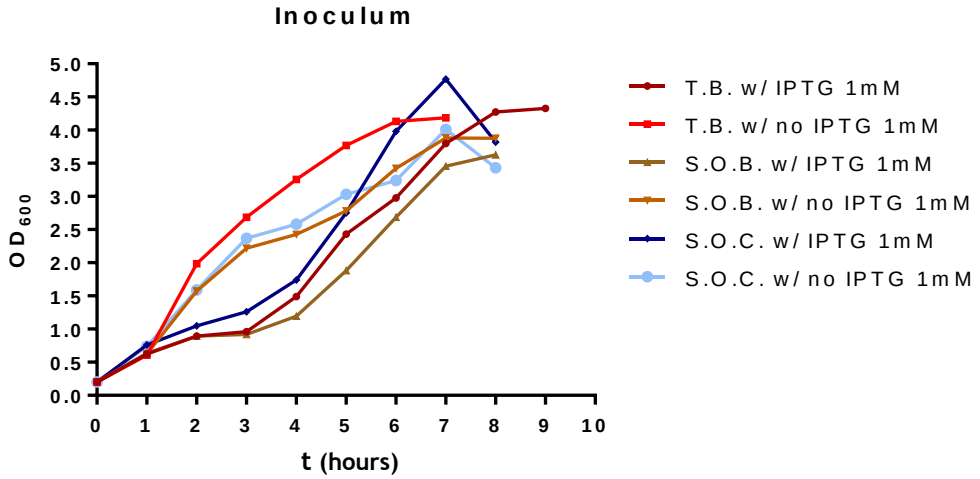

Figure 9: A direct comparison between *E. coli* BL21 (DE3) growth profile in TB, SOB and SOC liquid culture media.

At this stage, it was also important to evaluate the presence of STEAP1 fragment in both pellet and supernatant in order to understand the protein compartmentalization. Thereby, as showed in figure 10, TB medium allowed higher overexpression of $STEAP1_{1-142}$, with a preferential location in membrane fraction. However, only basal expression levels were observed in cell supernatant. The most interesting and relevant results came from the absence of $STEAP1_{1-142}$ levels in IPTG induced media, in contrast with no induced trials, where a stable protein pattern was obtained as excepted, with a band between 17-25 kDa molecular weight, which corroborate with previous data concerning the biosynthesis without induction of integral membrane chaperone (YidC) and the glutamate proton symporter (GltP) (130). The relative quantification of $STEAP1_{1-142}$ was estimated by densitometry.

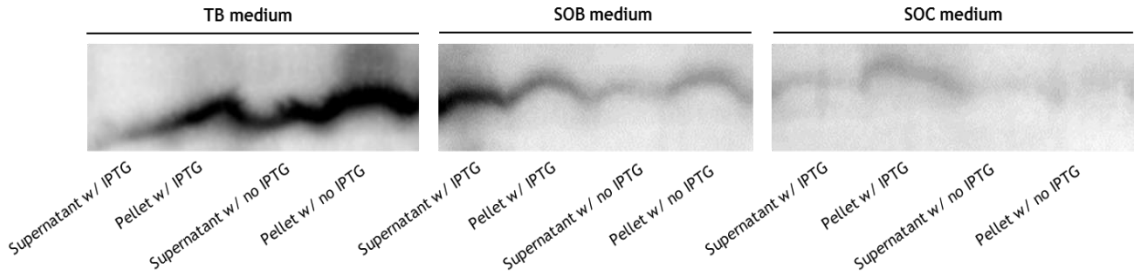

Figure 10: Western blot analysis of human $STEAP1_{1-142}$ peptide production and cellular compartmentalization in TB, SOC and SOC liquid culture media during the biosynthesis process, under the presence (w/ – with) and absence (w/ no – without) of inducer IPTG.

However, preceding studies reported that lactose could also be used as an alternative inducer, even presenting increased yields of membrane proteins production in comparison with those achieved with IPTG (131, 132). Therefore, the overall process described above was repeated in TB medium, adding Lactose at 1 mM as main inducer. Herein, the results indicated a shorter fermentation period and lower OD_{600} values, in comparison with those obtained for IPTG or non-induced cultures. This can be explained due to toxic effects on the host internal environment

caused by the expression of genes encoding the target protein, which negatively affect biomass formation and proteins production (130). Furthermore, from the analysis of figure 11 the presence of a 17-25 kDa protein in non-induced extracts was revealed, agreeing with the expected molecular weight and clearly proved that culturing *E. coli* BL21 (DE3) cells in TB medium omitting IPTG or Lactose induction lead to a most effective and increased STEAP1$_{1-142}$ production, besides providing a cost-effective and innovative alternative for membrane proteins biosynthesis (130, 133, 134).

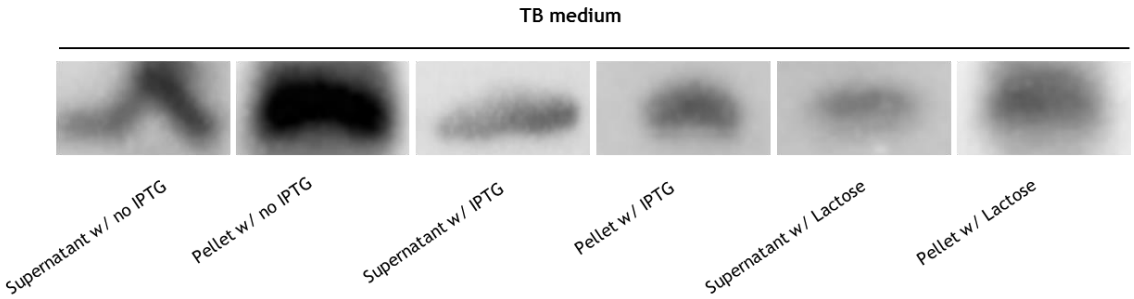

Figure 11: Western blot analysis of human STEAP1$_{1-142}$ production in TB medium, in the presence of lactose inducer and an integrated comparison with IPTG induce (w/ – with) and non-induced (w/ no – without) cultures.

In order to understand when STEAP1$_{1-142}$ attained highest production, considering the overall fermentation time, additional experiments in TB medium without adding any inducer were performed at 37 ºC and 250 rpm, but with the particularity of collecting samples in time intervals of 2 h during 12 h. In this case, higher OD_{600} values (OD_{600} = 7.0 at 12 h) were achieved, may be due to less interferences induced on the system. Moreover, as seen in figure 12A, STEAP1$_{1-142}$ expression was strongly detected in the interval between 6 to 8 h of fermentation by a progressive increase in the band density, after which was verified a decrease in intensity. The culture temperature, pH and stirring rate are parameters that influence protein biosynthesis. Therefore, these conditions were previously optimized aiming the production of human soluble proteins, for example catecol O-metiltransferase (COMT) in complex media, where is included TB (122, 135, 136). So, in order to access the most favorable physical parameters for STEAP1$_{1-142}$ overexpression, we modified the culture conditions from 37 ºC, pH 7.2 and 250 rpm to a temperature of 35 ºC, pH 6.2 and stirring rate of 351 rpm. The figure 12B demonstrated that, in fact, the peptide production was more accentuated near 8 h, corroborating our previous results and establish the ideal fermentation stop period in order to perform the STEAP1$_{1-142}$ recuperation.

Considering synergic interactions between the physic parameters described above and their effects over mass productivity and volumetry of target protein, an optimization of these conditions was also performed for semi-defined medium. It seemed an attractive option for membrane protein biosynthesis in previous trials, wherein it was presented a double rate bacterial growth and easier downstream processing, in comparison with complex medium (122,

135). So, STEAP1$_{1-142}$ biosynthesis in semi-defined medium with glycerol as the main carbon source at 35 ºC, 351 rpm and pH 6.2 was assessed. However, *E. coli* in the pre inoculum medium showed an extremely slow growth rate and the OD_{600} values demonstrated a stagnation or premature death of these cells, which not correspond to our interests and did not allow more detailed studies.

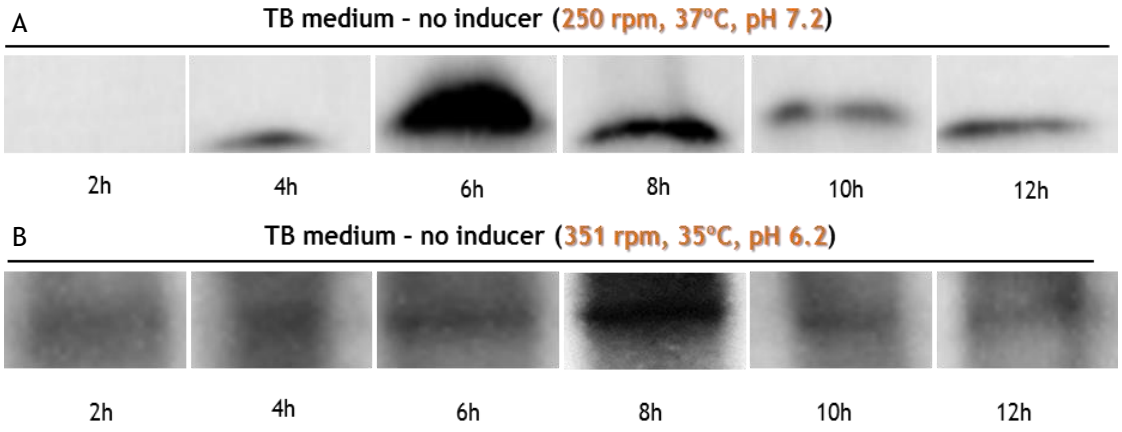

Figure 12: A: Western blot analysis of STEAP1$_{1-142}$ production in TB medium, omitting the addition of an inducer, in time intervals of 2 h during 12 h; B: Western blot analysis of STEAP1$_{1-142}$ production in TB medium, omitting the addition of an inducer, in time intervals of 2 h during 12 h, using fermentation conditions previously described as ideal (351 rpm, 35 ºC and pH 6.2).

3. STEAP1 solubilization

A proper isolation process for further structural, functional and biointeraction analysis has a main importance to obtain a complete characterization of membrane proteins in order to understand the 3D-native structure and then generate drugs that target specific sites within the target protein (137, 138). However, between purified and biochemically identified proteins, less than 2% of the 3D structures listed in the protein data bank are transmembrane or membrane proteins, due to the existing challenges associated with solubilization and purification, in considerable amounts for crystallization. This is mainly owed to their presence in low levels and being embedded in the lipid bilayer, which require the use of detergents (125, 138, 139). Therefore, the solubilization process is crucial for counter the natural tendency of transmembrane proteins to aggregate and then improve the yield of target protein (125, 139).

The recovery of membrane proteins requires the disruption of the host cell wall. Several methods are usually applied to *E. coli* lysis, including glass beads, considered the simplest method and the most suitable for lab-scale cell disruption, since it can maintain the stability of target protein (123, 140, 141). The main principle consists in vortexing the cells, combined with lysis buffer and glass beads, for 7 cycles of 1 min with an interval of 1 min on ice, in a procedure optimized for another membrane protein by our research team (123). Moreover, lysozyme, a lytic enzyme, was added to help in cell wall degradation and consequently to release intracellular proteins. In turn, DNAse was also used to digest nucleic acids, in order to

avoid the negative effect of the released of long nucleic acid chains during the disruption process, which promote an undesirable viscosity in the lysis extracts (142, 143).

Concerning membrane proteins, it is important to transfer them to a hydrophobic environment to resemble the native lipid bilayer. This is accomplished treating the lysis extract with a proper detergent, consisting in amphipathic molecules with a polar head group and an hydrophobic chain that adhere to the hydrophobic regions of target proteins and resolubilize them from the membrane (126, 138, 144, 145). Consequently, the selection of the right detergent is crucial for proper isolation and purification of target membrane protein (126, 145).

Therefore, it was evaluated the effect of different detergents in STEAP1$_{1-142}$ recovery with 1 % (v/v), including three non-ionic (Tween-20, Triton X-100 and Digitonin), one ionic (SDS) and one zwitterionic (CHAPS). The samples came from a TB medium liquid culture, deprived of an inducer, performed at 37 ºC and 250 rpm and the respective pellets resulting from cell lysis were resolubilized overnight at 4 ºC. As reported in figure 13, SDS was not effective in solubilize STEAP1$_{1-142}$ and also promoted a significant denaturation in lower molecular weight contaminants. In turn, Tween-20, Digitonin and CHAPS showed weak STEAP1$_{1-142}$ expression and thus were not considered efficient in this step. Interestingly, Triton X-100 achieved most effective results, maintaining STEAP1$_{1-142}$ native structure with higher expression patterns, in comparison with the control sample. However, it was noted the presence of several impurities, as a consequence of the mechanical lysis process, which demands an appropriated separation strategy in order to obtain a fully purified STEAP1$_{1-142}$ peptide for biointeraction and structural studies.

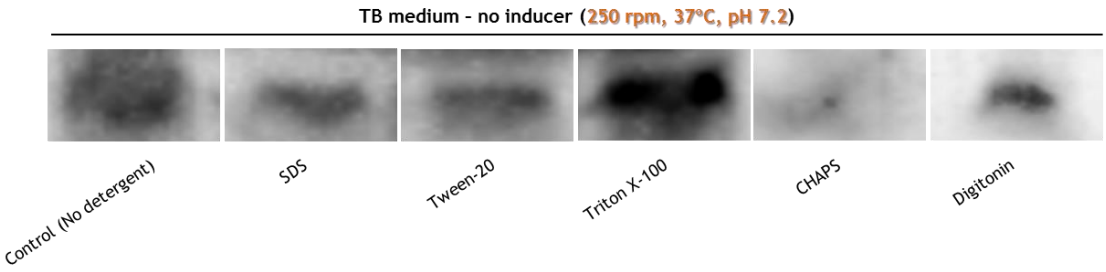

Figure 13: Western blot analysis of the STEAP1$_{1-142}$ recovery using 1 % (v/v) of several common detergents in the resolubilization of the target protein membrane fraction.

4. STEAP1 purification by an immobilized metal affinity chromatography

Once established the host strain, culture medium, fermentation conditions, lysis method and detergent that allow to obtain higher expression levels of STEAP1$_{1-142}$, a suitable purification process should be conducted. Briefly, the purification methods are divided in two distinct categories, namely techniques that exploit the intrinsic properties of the protein and those that require the presence of a fusion tag (125, 137). The fusion tag-based methods are the most popular and a proper choice for express and purify transmembrane proteins, mainly those that

enable immobilized metal affinity chromatography (IMAC). This technique has been widely used in the recent decade at laboratory scale for the isolation of proteins from fermentation broths solubilized with ionic or nonionic detergents, since it presents a high dynamic binding capacity and a desirable selectivity (125, 138, 146).

The $STEAP1_{1-142}$ peptide contains a His-tag, also known as 6xHis-tag, which is a small purification tag composed by six or more consecutive histidine residues that do not introduce considerable changes in protein conformation, besides increasing its expression in heterologous expression systems (138, 147). IMAC is frequently used as a first step during purification of His-tagged proteins. This technique can be used under denaturing conditions, since the His-tag does not require a specific structural conformation for binding to immobilized metals, besides the high binding capacity, low cost and easy cleaning (147).

Concerning this study, initial trials were conducted using a nickel resin to understand the chromatographic behavior of $STEAP1_{1-142}$. The binding of the protein to the matrix was performed using a binding buffer with 500 mM NaCl, 50 mM Tris-base, 1 mM $MgCl_2$ and 5 mM Imidazole at pH 7.8. At low concentrations in the binding buffer,imidazole competes with ions charged in the columns and prevents the binding of host proteins with histidine tails to the matrix. Therefore, it is possible to elute target proteins and simultaneously remove completely the contaminants during sample injection (148). Consequently, an increasing linear gradient of elution buffer containing 500 mM imidazole was tested in order to assess the imidazole concentration necessary to elute $STEAP1_{1-142}$.

As seen in figure 14, the chromatographic profile showed only two peaks of interest. A western blot analysis was carried out to confirm the immunological activity of the protein and it was confirmed the presence of $STEAP1_{1-142}$ immunodomain single band with correct molecular weight 17-25 kDa in the purified fraction correspondent to peak II. Also, a clean lane was observed for peak I, meaning that nickel column was capable to bind almost completely the injected protein. A SDS-PAGE was performed in order to confirm if the nickel column presented the desired selectivity to totally separate $STEAP1_{1-142}$ using Comassie staining. However, considerable amounts of high molecular weight contaminants were still interfering with our main purpose of obtaining a completely purified fragment. Therefore, an alternative strategy was adopted, which consisted in charge IMAC columns with cobalt resin.

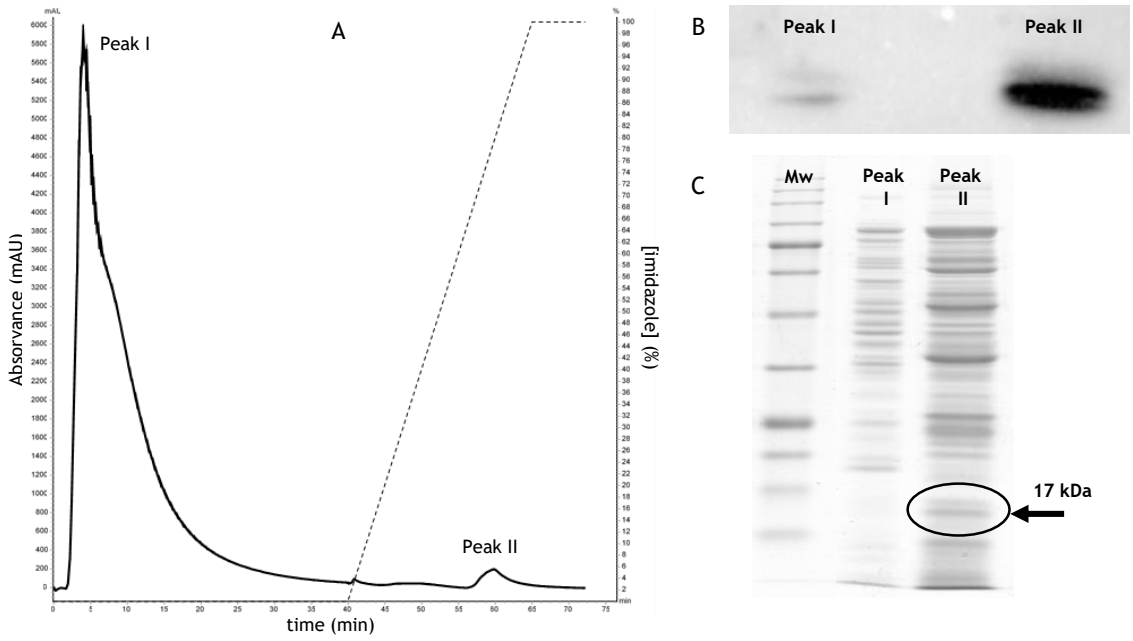

Figure 14: A: Chromatographic profile of STEAP1$_{1-142}$ purification from E. *coli* lysates on a HisTrap FF crude (5 mL column volume) with nickel ions immobilized; B: Western blot/SDS-PAGE analysis of collected fractions. STEAP1$_{1-142}$ position in the western blot gel is at the correct position (17-25 kDa); C: STEAP1$_{1-142}$ fraction in SDS-PAGE gel (Comassie staining) is represented by an arrow. Blank line represents absorbance at 280 nm, while dashed line the imidazole concentration. Binding process was performed at 50 mM imidazole at 0.5 mL/min flow rate followed by an increasing elution linear gradient to 500 mM imidazole at 1.0 mL/min flow rate. A final step at 500 mM imidazole, 500 mM NaCl, 50 mM Tris and 1 mM $MgCl_2$ buffer at pH 7.8 and 1.0 mL/ min flow rate was also performed.

It was reported that cobalt resins have lower affinity for polyhistidine affinity tag, less nonspecific protein binding compared to nickel charged columns, which result in higher elution product purity and reduced metal contamination (149, 150). Moreover, cobalt offers desirable characteristics such as stability of separated protein, high loading, mild elution conditions, simple regeneration and low cost. This fact lead us to test this procedure in order to compare the effects concerning STEAP1$_{1-142}$ isolation with those obtained for nickel columns (149). Besides, cobalt IMAC was previously optimized using a binding buffer containing low levels of imidazole, coinciding with our project (151).

The chromatographic profile in cobalt resins were conducted in the same conditions referred for nickel. The binding of the protein to the matrix was performed using the same binding buffer and an increasing linear gradient of elution buffer containing 500 mM imidazole was applied along with a final step to totally elute compounds with higher affinity for the column. Since cobalt matrix present reduced binding affinity in comparison with nickel ones, it was expected that STEAP1$_{1-142}$ elution peak appeared at lower percentage of imidazole, considering that less amount of competitive agent is necessary to elute our protein. In fact, the chromatographic profile of STEAP1$_{1-142}$ was similar to those obtained in previous assays, only with two peaks of interest. This result was very important since it allowed to establish a characteristic chromatogram and enable a tighter control of STEAP1$_{1-142}$ behavior when linear gradient is used, as seen in figure 15.

Moreover, it was once again observed a clean lane for peak I as an evidence that cobalt column was capable to completely bind the injected protein, even with less capacity comparing to nickel. Furthermore, a single band corresponding to STEAP1$_{1-142}$ immunodomain at correct molecular weight was observed in western blot analysis in the elution fraction correspondent to peak II, demonstrating that both tested resins were capable to firstly totally bind the protein with a single fraction. Also, as a consequence of reduced binding capacity inherent to cobalt matrix, it was expected higher selectivity for STEAP1$_{1-142}$ and less amount of contaminants. For that, a SDS-PAGE was conducted to prove if the cobalt column presented the necessary selectivity to totally separate STEAP1$_{1-142}$ by using Comassie staining.

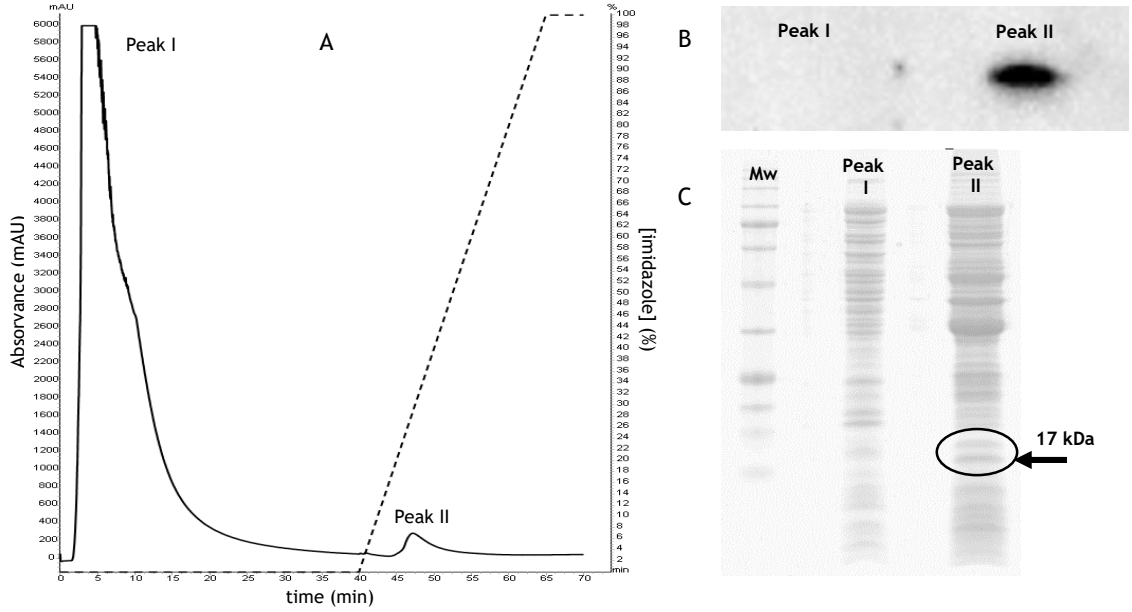

Figure 15: A: Chromatographic profile of STEAP1$_{1-142}$ purification from *E. coli* lysates on a HisTrap FF crude (5 mL column volume) with cobalt ions immobilized; B: Western blot/SDS-PAGE analysis of collected fractions. STEAP1$_{1-142}$ position in the western blot gel is at the correct position (17-25 kDa); C: STEAP1$_{1-142}$ fraction in SDS-PAGE gel (Comassie staining) is represented by an arrow. Blank line represents absorbance at 280 nm, while dashed line the imidazole concentration. Binding process was performed at 50 mM imidazole at 0.5 mL/min flow rate followed by an increasing elution linear gradient to 500 mM imidazole at 1.0 mL/min flow rate. A final step at 500 mM imidazole, 500 mM NaCl, 50 mM Tris and 1 mM $MgCl_2$ buffer at pH 7.8 and 1.0 mL/ min flow rate was also observed.

Despite a considerable amount of contaminants were eluted in peak I and then separated from the sample, it was not possible yet to obtain a completely purified band in peak II, which invalidate the development of biointeraction and structural complementary studies. Consequently, another strategy should be employed in order to achieve a fully purified STEAP1$_{1-142}$ peptide.

Chapter 4

Conclusion and Future Perspectives

Currently, the knowledge of transmembrane proteins biosynthesis is crucial due to its role in the development of novel therapeutic tools for several human pathologies. Therefore, it is essential improve the currently applied strategies or create new ones in order to increase the yield of production and purpose new purification strategies. Then, it will be possible to obtain significant quantities of proteins and perform biointeraction and structural studies.

The recombinant expression system used in this work harboring a plasmid pET101/D-STEAP1$_{1-142}$ allowed an efficient production of target protein in an immunological form. Herein, it was defined TB culture medium as the most suitable for E. *coli* BL21(DE3) as well as the adequate temperature, pH and orbital stirring conditions, namely 37 ºC, 7.2 and 250 rpm, respectively. Unlike great majority of published studies, it was possible to produce STEAP1$_{1-142}$ omitting an inducer, since the expression levels were reduced in IPTG and lactose trials. Also, STEAP1$_{1-142}$ cellular location was defined to be majority present in pellets instead of supernatants.

As membrane protein, the recovery step was done easily by solubilization with 1 % (v/v) of a non-ionic detergent, Triton X-100, since it demonstrated to be the most suitable between other four tested and promoted high levels of recovery. However, different detergent concentration must be tested in the future because it is a parameter that highly influence the recuperation step. Alternative systems capable to create a hydrophobic surrounding environment, such as bicelles, reverse-micelles or nanolipoproteins and resemble the native lipid bilayer in a more efficiently manner in comparison with detergents could also be experienced. The application of an ultracentrifugation step after membrane solubilization should be applied with the purpose to remove several contaminants, which could interfere with the downstream stage.

The secretion of STEAP1$_{1-142}$ coupled with a His-tag proved to be advantageous by allowed most efficient purification strategies, namely affinity chromatography approaches. The chromatographic profile obtained from the two tested columns charged with nickel and cobalt were similar, showing only two peaks of interest. A single immunoreactive fraction was obtained in western-blot analysis in the eluted peak, however the SDS-PAGE comassie staining demonstrated a considerable background of contaminants. Therefore, it is important to improve this method, initially by adopting a step elution gradient to precisely define in which moment STEAP1$_{1-142}$ is eluted in a more purified fraction, employing a pre-purification approach to eliminate other interfering compounds or polish the target fraction by ionic exchange chromatography.

References

1. Powers GL, Marker PC. Recent advances in prostate development and links to prostatic diseases. Wiley Interdisciplinary Reviews: Systems Biology and Medicine. 2013;5(2):243-56.
2. Hammerich KH, Ayala GE, Wheeler TM. Anatomy of the prostate gland and surgical pathology of prostate cancer. Cambridge University, Cambridge. 2009:1-10.
3. Wong Y, Wang X, Ling M. Prostate development and carcinogenesis. International review of cytology. 2003;227:65-130.
4. Hayward SW, Cunha GR. The prostate: development and physiology. Radiologic Clinics of North America. 2000;38(1):1-14.
5. Zhou Y, Bolton EC, Jones JO. Androgens and androgen receptor signaling in prostate tumorigenesis. Journal of molecular endocrinology. 2015;54(1):R15-R29.
6. Sooriakumaran P, Sievert K-D, Srivastava A, Tewari A. Applied Anatomy of the Prostate. 2012.
7. Ho CK, Habib FK. Estrogen and androgen signaling in the pathogenesis of BPH. Nature Reviews Urology. 2011;8(1):29-41.
8. Davis JN, Day ML. The convergence of hormone regulation and cell cycle in prostate physiology and prostate tumorigenesis. Molecular biotechnology. 2002;22(2):129-38.
9. Fine SW, Reuter VE. Anatomy of the prostate revisited: implications for prostate biopsy and zonal origins of prostate cancer. Histopathology. 2012;60(1):142-52.
10. Lee CH, Akin-Olugbade O, Kirschenbaum A. Overview of prostate anatomy, histology, and pathology. Endocrinology and metabolism clinics of North America. 2011;40(3):565-75.
11. Selman SH. The McNeal prostate: a review. Urology. 2011;78(6):1224-8.
12. McLaughlin PW, Troyer S, Berri S, Narayana V, Meirowitz A, Roberson PL, et al. Functional anatomy of the prostate: implications for treatment planning. International Journal of Radiation Oncology* Biology* Physics. 2005;63(2):479-91.
13. McNeal JE. Anatomy of the prostate and morphogenesis of BPH. Progress in clinical and biological research. 1984;145:27.
14. Timms BG. Prostate development: a historical perspective. Differentiation. 2008;76(6):565-77.
15. McNeal J. Regional morphology and pathology of the prostate. American journal of clinical pathology. 1968;49(3):347.
16. McNeal JE. Origin and evolution of benign prostatic enlargement. Investigative urology. 1978;15(4):340-5.
17. Siegel R, Naishadham D, Jemal A. Cancer statistics, 2013. CA: a cancer journal for clinicians. 2013;63(1):11-30.

18. Ferlay J, Soerjomataram I, Dikshit R, Eser S, Mathers C, Rebelo M, et al. Cancer incidence and mortality worldwide: sources, methods and major patterns in GLOBOCAN 2012. International journal of cancer. 2015;136(5):E359-E86.
19. Attard G, Parker C, Eeles RA, Schröder F, Tomlins SA, Tannock I, et al. Prostate cancer. The Lancet. 2016;387(10013):70-82.
20. Alvarez-Cubero MJ, Saiz M, Martinez-Gonzalez LJ, Alvarez JC, Lorente JA, Cozar JM, editors. Genetic analysis of the principal genes related to prostate cancer: a review. Urologic Oncology: Seminars and Original Investigations; 2013: Elsevier.
21. Bostwick DG, Burke HB, Djakiew D, Euling S, Ho Sm, Landolph J, et al. Human prostate cancer risk factors. Cancer. 2004;101(S10):2371-490.
22. Potosky AL, Miller BA, Albertsen PC, Kramer BS. The role of increasing detection in the rising incidence of prostate cancer. Jama. 1995;273(7):548-52.
23. Gomes IM, Arinto P, Lopes C, Santos CR, Maia CJ, editors. STEAP1 is overexpressed in prostate cancer and prostatic intraepithelial neoplasia lesions, and it is positively associated with Gleason score. Urologic Oncology: Seminars and Original Investigations; 2014: Elsevier.
24. Witte JS. Prostate cancer genomics: towards a new understanding. Nature reviews Genetics. 2009;10(2):77-82.
25. Ihlaseh-Catalano SM, Drigo SA, Jesus C, Domingues MAC, Trindade Filho JCS, Camargo JLV, et al. STEAP1 protein overexpression is an independent marker for biochemical recurrence in prostate carcinoma. Histopathology. 2013;63(5):678-85.
26. Miller DC, Hafez KS, Stewart A, Montie JE, Wei JT. Prostate carcinoma presentation, diagnosis, and staging. Cancer. 2003;98(6):1169-78.
27. Romanuik TL, Wang G, Morozova O, Delaney A, Marra MA, Sadar MD. LNCaP Atlas: gene expression associated with in vivo progression to castration-recurrent prostate cancer. BMC medical genomics. 2010;3(1):1.
28. Frantz C, Stewart KM, Weaver VM. The extracellular matrix at a glance. Journal of cell science. 2010;123(24):4195-200.
29. Duffy M, McGowan P, Gallagher W. Cancer invasion and metastasis: changing views. The Journal of pathology. 2008;214(3):283-93.
30. Brand LJ, Dehm SM. Androgen receptor gene rearrangements: new perspectives on prostate cancer progression. Current drug targets. 2013;14(4):441.
31. Shafi AA, Yen AE, Weigel NL. Androgen receptors in hormone-dependent and castration-resistant prostate cancer. Pharmacology & therapeutics. 2013;140(3):223-38.
32. Luu-The V, Bélanger A, Labrie F. Androgen biosynthetic pathways in the human prostate. Best Practice & Research Clinical Endocrinology & Metabolism. 2008;22(2):207-21.
33. Marks LS, Mostaghel EA, Nelson PS. Prostate tissue androgens: history and current clinical relevance. Urology. 2008;72(2):247-54.
34. Clinckemalie L, Vanderschueren D, Boonen S, Claessens F. The hinge region in androgen receptor control. Molecular and cellular endocrinology. 2012;358(1):1-8.

35. Dehm SM, Tindall DJ. Androgen receptor structural and functional elements: role and regulation in prostate cancer. Molecular endocrinology. 2007;21(12):2855-63.
36. Suzuki H, Ueda T, Ichikawa T, Ito H. Androgen receptor involvement in the progression of prostate cancer. Endocrine-related cancer. 2003;10(2):209-16.
37. Egan A, Dong Y, Zhang H, Qi Y, Balk SP, Sartor O. Castration-resistant prostate cancer: adaptive responses in the androgen axis. Cancer treatment reviews. 2014;40(3):426-33.
38. Saraon P, Jarvi K, Diamandis EP. Molecular alterations during progression of prostate cancer to androgen independence. Clinical chemistry. 2011;57(10):1366-75.
39. Pienta KJ, Bradley D. Mechanisms underlying the development of androgen-independent prostate cancer. Clinical Cancer Research. 2006;12(6):1665-71.
40. Wen S, Niu Y, Lee SO, Chang C. Androgen receptor (AR) positive vs negative roles in prostate cancer cell deaths including apoptosis, anoikis, entosis, necrosis and autophagic cell death. Cancer treatment reviews. 2014;40(1):31-40.
41. Heinlein CA, Chang C. Androgen receptor in prostate cancer. Endocrine reviews. 2004;25(2):276-308.
42. Yu S-Q, Lai K-P, Xia S-J, Chang H-C, Chang C, Yeh S. The diverse and contrasting effects of using human prostate cancer cell lines to study androgen receptor roles in prostate cancer. Asian J Androl. 2009;11(1):39-48.
43. Brooke GN, Bevan C. The role of androgen receptor mutations in prostate cancer progression. Current genomics. 2009;10(1):18-25.
44. McPhaul MJ. Mechanisms of prostate cancer progression to androgen independence. Best Practice & Research Clinical Endocrinology & Metabolism. 2008;22(2):373-88.
45. Culig Z, Santer FR. Androgen receptor signaling in prostate cancer. Cancer and Metastasis Reviews. 2014;33(2-3):413-27.
46. Cai C, Chen S, Ng P, Bubley GJ, Nelson PS, Mostaghel EA, et al. Intratumoral de novo steroid synthesis activates androgen receptor in castration-resistant prostate cancer and is upregulated by treatment with CYP17A1 inhibitors. Cancer research. 2011;71(20):6503-13.
47. Mellado B, Codony J, Ribal MJ, Visa L, Gascón P. Molecular biology of androgen-independent prostate cancer: the role of the androgen receptor pathway. Clinical and Translational Oncology. 2009;11(1):5-10.
48. Locke JA, Guns ES, Lubik AA, Adomat HH, Hendy SC, Wood CA, et al. Androgen levels increase by intratumoral de novo steroidogenesis during progression of castration-resistant prostate cancer. Cancer research. 2008;68(15):6407-15.
49. Bunting PS. A guide to the interpretation of serum prostate specific antigen levels. Clinical biochemistry. 1995;28(3):221-41.
50. Izumi K, Lin W-J, Miyamoto H, Huang C-K, Maolake A, Kitagawa Y, et al. Outcomes and predictive factors of prostate cancer patients with extremely high prostate-specific antigen level. Journal of cancer research and clinical oncology. 2014;140(8):1413-9.
51. Ladjevardi S, Berglund A, Varenhorst E, Bratt O, Widmark A, Sandblom G. Treatment with curative intent and survival in men with high-risk prostate cancer. A population-based

study of 11 380 men with serum PSA level 20–100 ng/mL. BJU international. 2013;111(3):381-8.

52. Wolf A, Wender RC, Etzioni RB, Thompson IM, D'Amico AV, Volk RJ, et al. American Cancer Society guideline for the early detection of prostate cancer: update 2010. CA: a cancer journal for clinicians. 2010;60(2):70-98.

53. Bussemakers MJ, van Bokhoven A, Verhaegh GW, Smit FP, Karthaus HF, Schalken JA, et al. DD3:: A New Prostate-specific Gene, Highly Overexpressed in Prostate Cancer. Cancer research. 1999;59(23):5975-9.

54. Filella X, Foj L, Milà M, Augé JM, Molina R, Jiménez W. PCA3 in the detection and management of early prostate cancer. Tumor Biology. 2013;34(3):1337-47.

55. Ferro M, Bruzzese D, Perdona S, Marino A, Mazzarella C, Perruolo G, et al. Prostate Health Index (Phi) and Prostate Cancer Antigen 3 (PCA3) significantly improve prostate cancer detection at initial biopsy in a total PSA range of 2–10 ng/ml. PLoS one. 2013;8(7):e67687.

56. Damber J-E, Aus G. Prostate cancer. The Lancet. 2008;371(9625):1710-21.

57. Cannata DH, Kirschenbaum A, Levine AC. Androgen deprivation therapy as primary treatment for prostate cancer. The Journal of Clinical Endocrinology & Metabolism. 2011;97(2):360-5.

58. Huggins C, Hodges CV. Studies on prostatic cancer: I. The effect of castration, of estrogen and of androgen injection on serum phosphatases in metastatic carcinoma of the prostate. The Journal of urology. 2002;167(2):948-51.

59. Kahn B, Collazo J, Kyprianou N. Androgen receptor as a driver of therapeutic resistance in advanced prostate cancer. Int J Biol Sci. 2014;10(6):588-95.

60. Karantanos T, Corn PG, Thompson TC. Prostate cancer progression after androgen deprivation therapy: mechanisms of castrate resistance and novel therapeutic approaches. Oncogene. 2013;32(49):5501-11.

61. Patel JC, Maughan BL, Agarwal AM, Batten JA, Zhang TY, Agarwal N. Emerging molecularly targeted therapies in castration refractory prostate cancer. Prostate cancer. 2013;2013.

62. Amaral TMS, Macedo D, Fernandes I, Costa L. Castration-resistant prostate cancer: mechanisms, targets, and treatment. Prostate cancer. 2012;2012.

63. Hu J, Hsu J, Bergerot PG, Yuh BE, Stein CA, Pal SK. Preoperative therapy for localized prostate cancer: a comprehensive overview. Maturitas. 2013;74(1):3-9.

64. Yap TA, Zivi A, Omlin A, de Bono JS. The changing therapeutic landscape of castration-resistant prostate cancer. Nature Reviews Clinical Oncology. 2011;8(10):597-610.

65. Dimakakos A, Armakolas A, Koutsilieris M. Novel tools for prostate cancer prognosis, diagnosis, and follow-up. BioMed research international. 2014;2014.

66. Hayashi T, Oue N, Sakamoto N, Anami K, Oo HZ, Sentani K, et al. Identification of transmembrane protein in prostate cancer by the *Escherichia coli* ampicillin secretion trap: expression of CDON is involved in tumor cell growth and invasion. Pathobiology. 2010;78(5):277-84.

67. Bradford TJ, Tomlins SA, Wang X, Chinnaiyan AM, editors. Molecular markers of prostate cancer. Urologic Oncology: Seminars and Original Investigations; 2006: Elsevier.
68. Gu Z, Thomas G, Yamashiro J, Shintaku I, Dorey F, Raitano A, et al. Prostate stem cell antigen (PSCA) expression increases with high gleason score, advanced stage and bone metastasis in prostate cancer. Oncogene. 2000;19(10).
69. Paul B, Dhir R, Landsittel D, Hitchens MR, Getzenberg RH. Detection of prostate cancer with a blood-based assay for early prostate cancer antigen. Cancer research. 2005;65(10):4097-100.
70. Varambally S, Dhanasekaran SM, Zhou M, Barrette TR, Kumar-Sinha C, Sanda MG, et al. The polycomb group protein EZH2 is involved in progression of prostate cancer. Nature. 2002;419(6907):624-9.
71. Shariat SF, Semjonow A, Lilja H, Savage C, Vickers AJ, Bjartell A. Tumor markers in prostate cancer I: blood-based markers. Acta Oncologica. 2011;50(sup1):61-75.
72. Yu J, Yu J, Mani R-S, Cao Q, Brenner CJ, Cao X, et al. An integrated network of androgen receptor, polycomb, and TMPRSS2-ERG gene fusions in prostate cancer progression. Cancer cell. 2010;17(5):443-54.
73. Pértega-Gomes N, Vizcaíno JR, Gouveia C, Jerónimo C, Henrique RM, Lopes C, et al. Monocarboxylate transporter 2 (MCT2) as putative biomarker in prostate cancer. The Prostate. 2013;73(7):763-9.
74. Vaz CV, Alves MG, Marques R, Moreira PI, Oliveira PF, Maia CJ, et al. Androgen-responsive and nonresponsive prostate cancer cells present a distinct glycolytic metabolism profile. The international journal of biochemistry & cell biology. 2012;44(11):2077-84.
75. Pértega-Gomes N, Vizcaíno JR, Miranda-Gonçalves V, Pinheiro C, Silva J, Pereira H, et al. Monocarboxylate transporter 4 (MCT4) and CD147 overexpression is associated with poor prognosis in prostate cancer. BMC cancer. 2011;11(1):1.
76. Grant CM, Kyprianou N. Epithelial mesenchymal transition (EMT) in prostate growth and tumor progression. Translational andrology and urology. 2013;2(3):202.
77. Anose BM, LaGoo L, Schwendinger J. Characterization of androgen regulation of ZEB-1 and PSA in 22RV1 prostate cancer cells. Hormonal Carcinogenesis V: Springer; 2008. p. 541-6.
78. Fritzsche FR, Jung M, Tölle A, Wild P, Hartmann A, Wassermann K, et al. ADAM9 expression is a significant and independent prognostic marker of PSA relapse in prostate cancer. European urology. 2008;54(5):1097-108.
79. Challita-Eid PM, Morrison K, Etessami S, An Z, Morrison KJ, Perez-Villar JJ, et al. Monoclonal antibodies to six-transmembrane epithelial antigen of the prostate-1 inhibit intercellular communication in vitro and growth of human tumor xenografts in vivo. Cancer research. 2007;67(12):5798-805.
80. Gomes IM, Maia CJ, Santos CR. STEAP proteins: from structure to applications in cancer therapy. Molecular Cancer Research. 2012;10(5):573-87.

81. Grunewald TG, Bach H, Cossarizza A, Matsumoto I. The STEAP protein family: versatile oxidoreductases and targets for cancer immunotherapy with overlapping and distinct cellular functions. Biology of the Cell. 2012;104(11):641-57.
82. Ohgami RS, Campagna DR, McDonald A, Fleming MD. The Steap proteins are metalloreductases. Blood. 2006;108(4):1388-94.
83. Gomes IM, Santos CR, Maia CJ. Expression of STEAP1 and STEAP1B in prostate cell lines, and the putative regulation of STEAP1 by post-transcriptional and post-translational mechanisms. Genes & cancer. 2014;5(3-4):142.
84. Hubert RS, Vivanco I, Chen E, Rastegar S, Leong K, Mitchell SC, et al. STEAP: a prostate-specific cell-surface antigen highly expressed in human prostate tumors. Proceedings of the National Academy of Sciences. 1999;96(25):14523-8.
85. Yang D, Holt GE, Velders MP, Kwon ED, Kast WM. Murine Six-Transmembrane Epithelial Antigen of the Prostate, Prostate Stem Cell Antigen, and Prostate-specific Membrane Antigen Prostate-specific Cell-Surface Antigens Highly Expressed in Prostate Cancer of Transgenic Adenocarcinoma Mouse Prostate Mice. Cancer research. 2001;61(15):5857-60.
86. Grunewald TG, Diebold I, Esposito I, Plehm S, Hauer K, Thiel U, et al. STEAP1 is associated with the invasive and oxidative stress phenotype of Ewing tumors. Molecular Cancer Research. 2012;10(1):52-65.
87. Ohgami RS, Campagna DR, Greer EL, Antiochos B, McDonald A, Chen J, et al. Identification of a ferrireductase required for efficient transferrin-dependent iron uptake in erythroid cells. Nature genetics. 2005;37(11):1264-9.
88. Yamamoto T, Tamura Y, Kobayashi J-i, Kamiguchi K, Hirohashi Y, Miyazaki A, et al. Six-transmembrane epithelial antigen of the prostate-1 plays a role for in vivo tumor growth via intercellular communication. Experimental cell research. 2013;319(17):2617-26.
89. Pan Y, Li Y, Guo L, Zhao Y, Zhao X. [Influence of expression of six transmembrane epithelial antigen of the prostate-1 on intracellular reactive oxygen species level and cell growth: an in vitro experiment]. Zhonghua yi xue za zhi. 2008;88(9):641-4.
90. Maia CJ, Socorro S, Schmitt F, Santos CR. STEAP1 is over-expressed in breast cancer and down-regulated by 17β-estradiol in MCF-7 cells and in the rat mammary gland. Endocrine. 2008;34(1-3):108-16.
91. Gomes IM, Santos CR, Socorro S, Maia CJ. Six transmembrane epithelial antigen of the prostate 1 is down-regulated by sex hormones in prostate cells. The Prostate. 2013;73(6):605-13.
92. Lalani E-N, Laniado ME, Abel PD. Molecular and cellular biology of prostate cancer. Cancer and Metastasis Reviews. 1997;16(1-2):29-66.
93. Valenti MT, Dalle Carbonare L, Bertoldo F, Donatelli L, Cascio VL. The effects on hTERT gene expression is an additional mechanism of amino-bisphosphonates in prostatic cancer cells. European journal of pharmacology. 2008;580(1):36-42.
94. Fromigue O, Kheddoumi N, Body J-J. Bisphosphonates antagonise bone growth factors' effects on human breast cancer cells survival. British journal of cancer. 2003;89(1):178-84.

95. Sewing L, Steinberg F, Schmidt H, Göke R. The bisphosphonate zoledronic acid inhibits the growth of HCT-116 colon carcinoma cells and induces tumor cell apoptosis. Apoptosis. 2008;13(6):782-9.
96. Brown JE, Neville-Webbe H, Coleman RE. The role of bisphosphonates in breast and prostate cancers. Endocrine-Related Cancer. 2004;11(2):207-24.
97. Valenti M, Giannini S, Donatelli L, Realdi G, Cascio VL, Dalle Carbonare L. Zoledronic acid decreases mRNA six-transmembrane epithelial antigen of prostate protein expression in prostate cancer cells. Journal of endocrinological investigation. 2010;33(4):244-9.
98. Wong P-F, Abubakar S. Comparative transcriptional study of the effects of high intracellular zinc on prostate carcinoma cells. Oncology reports. 2010;23(6):1501-16.
99. Yan M, Song Y, Wong CP, Hardin K, Ho E. Zinc deficiency alters DNA damage response genes in normal human prostate epithelial cells. The Journal of nutrition. 2008;138(4):667-73.
100. Costello L, Feng P, Milon B, Tan M, Franklin R. Role of zinc in the pathogenesis and treatment of prostate cancer: critical issues to resolve. Prostate cancer and prostatic diseases. 2004;7(2):111-7.
101. Doran MG, Watson PA, Cheal SM, Spratt DE, Wongvipat J, Steckler JM, et al. Annotating STEAP1 regulation in prostate cancer with 89Zr immuno-PET. Journal of Nuclear Medicine. 2014;55(12):2045-9.
102. Lu S, Tan Z, Wortman M, Dong Z. Regulation of heat shock protein 70-1 expression by androgen receptor and its signaling in human prostate cancer cells. International journal of oncology. 2010;36(2):459-67.
103. Machlenkin A, Paz A, Haim EB, Goldberger O, Finkel E, Tirosh B, et al. Human CTL epitopes prostatic acid phosphatase-3 and six-transmembrane epithelial antigen of prostate-3 as candidates for prostate cancer immunotherapy. Cancer research. 2005;65(14):6435-42.
104. Rodeberg DA, Nuss RA, Elsawa SF, Celis E. Recognition of six-transmembrane epithelial antigen of the prostate–expressing tumor cells by peptide antigen–induced cytotoxic T lymphocytes. Clinical cancer research. 2005;11(12):4545-52.
105. Alves PM, Faure O, Graff-Dubois S, Cornet S, Bolonakis I, Gross D-A, et al. STEAP, a prostate tumor antigen, is a target of human CD8+ T cells. Cancer Immunology, Immunotherapy. 2006;55(12):1515-23.
106. Gomella L, Nabhan C, DeVries T, Whitmore J, Frohlich M, George D. 683 Estimating the overall survival benefit of sipuleucel-T in the impact trial accounting for crossover treatment in control subjects with autologous immunotherapy generated from cyropreserved cells. The Journal of Urology. 2012;187(4):e278-e9.
107. Kantoff PW, Higano CS, Shore ND, Berger ER, Small EJ, Penson DF, et al. Sipuleucel-T immunotherapy for castration-resistant prostate cancer. New England Journal of Medicine. 2010;363(5):411-22.
108. Cole G, McCaffrey J, Ali AA, McCarthy HO. DNA vaccination for prostate cancer: key concepts and considerations. Cancer nanotechnology. 2015;6(1):1-23.
109. Liu M. DNA vaccines: a review. Journal of internal medicine. 2003;253(4):402-10.

110. Krupa M, Canamero M, Gomez CE, Najera JL, Gil J, Esteban M. Immunization with recombinant DNA and modified vaccinia virus Ankara (MVA) vectors delivering PSCA and STEAP1 antigens inhibits prostate cancer progression. Vaccine. 2011;29(7):1504-13.
111. de la Luz Garcia-Hernandez M, Gray A, Hubby B, Kast WM. In vivo effects of vaccination with six-transmembrane epithelial antigen of the prostate: a candidate antigen for treating prostate cancer. Cancer research. 2007;67(3):1344-51.
112. Boswell CA, Mundo EE, Zhang C, Bumbaca D, Valle NR, Kozak KR, et al. Impact of drug conjugation on pharmacokinetics and tissue distribution of anti-STEAP1 antibody–drug conjugates in rats. Bioconjugate chemistry. 2011;22(10):1994-2004.
113. Dong H, Zhu G, Tamada K, Chen L. B7-H1, a third member of the B7 family, co-stimulates T-cell proliferation and interleukin-10 secretion. Nature medicine. 1999;5(12):1365-9.
114. Weiner GJ, editor Picking the optimal target for antibody-drug conjugates2013: American Society of Clinical Oncology.
115. Weiner LM, Carter P. Tunable antibodies. Nature biotechnology. 2005;23(5):556-7.
116. Patching SG. Surface plasmon resonance spectroscopy for characterisation of membrane protein–ligand interactions and its potential for drug discovery. Biochimica et Biophysica Acta (BBA)-Biomembranes. 2014;1838(1):43-55.
117. Whitford D. Proteins: structure and function: John Wiley & Sons; 2013.
118. Goldflam M, Tarragó T, Gairí M, Giralt E. NMR studies of protein–ligand interactions. Protein NMR techniques. 2012:233-59.
119. Angulo J, Nieto PM. STD-NMR: application to transient interactions between biomolecules—a quantitative approach. European Biophysics Journal. 2011;40(12):1357-69.
120. Greenfield NJ. Using circular dichroism spectra to estimate protein secondary structure. Nature protocols. 2006;1(6):2876-90.
121. Smyth M, Martin J. x Ray crystallography. Journal of Clinical Pathology. 2000;53(1):8.
122. Silva R, Ferreira S, Bonifacio M, Dias J, Queiroz J, Passarinha L. Optimization of fermentation conditions for the production of human soluble catechol-O-methyltransferase by *Escherichia coli* using artificial neural network. Journal of biotechnology. 2012;160(3):161-8.
123. Pedro A, Oppolzer D, Bonifácio M, Maia C, Queiroz J, Passarinha L. Evaluation of MutS and Mut+ Pichia pastoris Strains for Membrane-Bound Catechol-O-Methyltransferase Biosynthesis. Applied biochemistry and biotechnology. 2015;175(8):3840-55.
124. Snijder HJA, Hakulinen J. Membrane Protein Production in E. coli for Applications in Drug Discovery. Advanced Technologies for Protein Complex Production and Characterization: Springer; 2016. p. 59-77.
125. Pandey A, Shin K, Patterson RE, Liu X-Q, Rainey JK. Current strategies for protein production and purification enabling membrane protein structural biology. Biochemistry and Cell Biology. 2016(ja).
126. Kubicek J, Block H, Maertens B, Spriestersbach A, Labahn J. Expression and purification of membrane proteins. Methods in enzymology. 2014;541(FZJ-2014-02986):117-40.

127. Löw C, Jegerschöld C, Kovermann M, Moberg P, Nordlund P. Optimisation of over-expression in E. coli and biophysical characterisation of human membrane protein synaptogyrin 1. PloS one. 2012;7(6):e38244.
128. Terpe K. Overview of bacterial expression systems for heterologous protein production: from molecular and biochemical fundamentals to commercial systems. Applied microbiology and biotechnology. 2006;72(2):211-22.
129. Flick K, Ahuja S, Chene A, Bejarano MT, Chen Q. Optimized expression of Plasmodium falciparum erythrocyte membrane protein 1 domains in *Escherichia coli*. Malaria journal. 2004;3(1):50.
130. Zhang Z, Kuipers G, Niemiec Ł, Baumgarten T, Slotboom DJ, de Gier J-W, et al. High-level production of membrane proteins in E. coli BL21 (DE3) by omitting the inducer IPTG. Microbial cell factories. 2015;14(1):1.
131. Li Z, Zhang X, Tan T. Lactose-induced production of human soluble B lymphocyte stimulator (hsBLyS) in E. coli with different culture strategies. Biotechnology letters. 2006;28(7):477-83.
132. Yan J, Zhao S-F, Mao Y-F, Luo Y-H. Effects of lactose as an inducer on expression of Helicobacter pylori rUreB and rHpaA, and *Escherichia coli* rLTKA63 and rLTB. World journal of gastroenterology: WJG. 2004;10(12):1755.
133. Nair R, Salvi P, Banerjee S, Raiker VA, Bandyopadhyay S, Soorapaneni S, et al. Yeast extract mediated autoinduction of lacUV5 promoter: an insight. New biotechnology. 2009;26(6):282-8.
134. Grossman TH, Kawasaki ES, Punreddy SR, Osburne MS. Spontaneous cAMP-dependent derepression of gene expression in stationary phase plays a role in recombinant expression instability. Gene. 1998;209(1):95-103.
135. Passarinha L, Bonifacio M, Queiroz J. Application of a fed-batch bioprocess for the heterologous production of hSCOMT in *Escherichia coli*. Journal of microbiology and biotechnology. 2009;19(9):972-81.
136. Passarinha L, Bonifácio M, Soares-da-Silva P, Queiroz J. A new approach on the purification of recombinant human soluble catechol-O-methyltransferase from an *Escherichia coli* extract using hydrophobic interaction chromatography. Journal of Chromatography A. 2008;1177(2):287-96.
137. Postis VG, Rawlings AE, Lesiuk A, Baldwin SA. Use of *Escherichia coli* for the Production and Purification of Membrane Proteins. Ion Channels: Methods and Protocols. 2013:33-54.
138. Lin S-H, Guidotti G. Purification of membrane proteins. Methods in enzymology. 2009;463:619-29.
139. Smith SM. Strategies for the purification of membrane proteins. Protein Chromatography: Methods and Protocols. 2011:485-96.
140. Benov L, Al-Ibraheem J. Disrupting *Escherichia coli*: a comparison of methods. Journal of biochemistry and molecular biology. 2002;35(4):428-31.

141. Song DD, Jacques NA. Cell Disruption of*Escherichia coli*by Glass Bead Stirring for the Recovery of Recombinant Proteins. Analytical biochemistry. 1997;248(2):300-1.
142. Ferreira S, Sousa F, Queiroz J, Domingues F. Improved recovery of a fusion protein containing the antigenic domain 1 of the human cytomegalovirus glycoprotein B. Biotechnology letters. 2005;27(16):1241-5.
143. Middelberg AP. Process-scale disruption of microorganisms. Biotechnology advances. 1995;13(3):491-551.
144. Pedro A, Bonifacio M, Queiroz J, Maia C, Passarinha L. A novel prokaryotic expression system for biosynthesis of recombinant human membrane-bound catechol-O-methyltransferase. Journal of biotechnology. 2011;156(2):141-6.
145. Seddon AM, Curnow P, Booth PJ. Membrane proteins, lipids and detergents: not just a soap opera. Biochimica et Biophysica Acta (BBA)-Biomembranes. 2004;1666(1):105-17.
146. Mooney JT, Fredericks DP, Zhang C, Christensen T, Jespergaard C, Schiødt CB, et al. Purification of a recombinant human growth hormone by an integrated IMAC procedure. Protein expression and purification. 2014;94:85-94.
147. Malhotra A. Tagging for protein expression. Methods in enzymology. 2009;463:239-58.
148. Fazen CH, Kahkoska AR, Doyle RP. Expression and purification of human PYY (3–36) in *Escherichia coli* using a His-tagged small ubiquitin-like modifier fusion. Protein expression and purification. 2012;85(1):51-9.
149. Zatloukalová E, Kučerová Z. Separation of cobalt binding proteins by immobilized metal affinity chromatography. Journal of Chromatography B. 2004;808(1):99-103.
150. Bornhorst JA, Falke JJ. [16] Purification of proteins using polyhistidine affinity tags. Methods in enzymology. 2000;326:245.
151. Camper DV, Viola RE. Fully automated protein purification. Analytical biochemistry. 2009;393(2):176-81.